8-2011

Stress relaxation of glass using a parallel plate viscometer

Guy-marie Vallet
Clemson University, guymarv@clemson.edu

STRESS RELAXATION OF GLASS USING A PARALLEL PLATE VISCOMETER

A Thesis
Presented to
The Graduate School of
Clemson University

In Partial Fulfillment
of the Requirements for the Degree of Master of Science
Materials Science and Engineering

By
Guy-Marie Vallet
August 2011

Accepted by:
Dr. Vincent Blouin, Committee Chair
Dr. Jean-Louis Bobet
Dr. Evelyne Fargin
Dr. Paul Joseph
Dr. Véronique Jubera
Dr. Igor Luzinov
Dr. Kathleen Richardson

ABSTRACT

Currently, grinding and polishing is the traditional method for manufacturing optical glass lenses. However, for a few years now, precision glass molding has gained importance for its flexibility in manufacturing aspheric lenses. With this new method, glass viscoelasticity and more specifically stress relaxation are important phenomena in the glass transition region to control the molding process and to predict the final lens shape.

The goal of this research is to extract stress relaxation parameters in shear of Pyrex® glass by using a Parallel Plate Viscometer (PPV). The PPV machine was originally created to measure the viscosity of glass solid cylinders by compression. It is used in this study for creep-recovery tests of glass samples. With this study we want to know if we are able to measure stress relaxation of glass using a helical spring geometry since it presents pure shear stress, for a temperature near the glass transition region (*i.e.*, 570°C). The results obtain with the PPV are post-processed using a finite term Prony series of a Generalized Maxwell model.

The additional goals of this study are to compare the results with those obtained by a previous student using a tensile creep apparatus, and to compare the experimental results with a numerical simulation using the finite element analysis software Abaqus.

ACKNOWLEDGMENTS

My first acknowledgments go to my advisor, Professor Vincent Blouin for his support, his advising, his good mood and to help me since the beginning with the grasp of English.

I would like to thank the Professor Kathleen Richardson for accepting me in the MILMI program and to make available her lab and the Parallel Plate Viscometer machine.

I owe my acknowledgments to my committee members from Clemson University: Prof. Paul Joseph and Prof. Igor Luzinov and from the Université de Bordeaux: Prof. Véronique Jubéra, Prof. Jean-Louis Bobet and Prof. Evelyne Fargin.

I want to express my gratitude to all my co-workers in the lab who help me in my research project and for the lively atmosphere in the office: Sylvain Danto, Peiman Mosaddegh, Dave Musgraves, Peter Wachtel, Guillaume Guery, Benn Gleason, Rémy Lestable, Spencer Novak, Christopher Ostrouchov, Taylor Shoulders, Daniel Thompson and Jacklyn Wilkinson.

Additionally I want to acknowledge the members of the exchange MILMI program for their continuous help with the administrative procedures: Adeline Barre, Leslie Bilger, Kathy Bolton and Emilie Journeau.

Finally, thanks to my family, my girlfriend and my friends who supported me from the other side of the Atlantic Ocean.

TABLE OF CONTENTS

Page

LIST OF TABLES

LIST OF FIGURES

CHAPTER ONE

INTRODUCTION

1.1 Research motivation

In precision glass molding, the stress relaxation properties of the glass are an important parameter for the shape accuracy of the lens. The molding process can be divided into four different steps shown in Figure 1.1. [1]

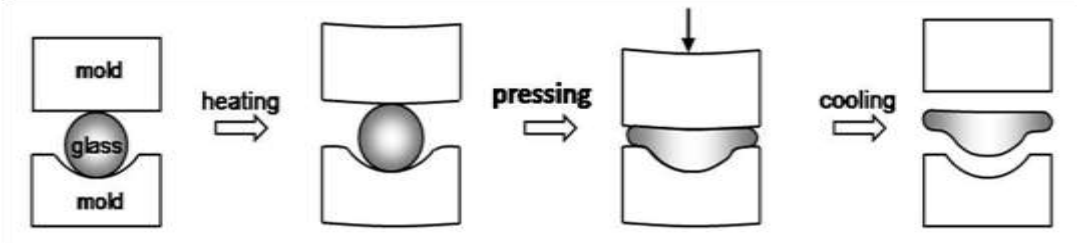

Step 1 Step 2 Step 3 Step 4

Figure 1.1. Precision glass molding process

During the first step, a glass preform is inserted between the two parts of the mold at room temperature. The second step consists of increasing the temperature into the glass transition region. During this step, the dimensions of the preform and the mold change slightly due to thermal expansion. In the third step which is called the compression step, the preform is compressed between the two molds to obtain the final shape of the lens. Finally, the fourth step consists of cooling the system to room temperature and releasing the lens. It is generally during the fourth step that stress

relaxation of the glass occurs. Material relaxation can lead to small deformations of the lens shape and to potentially harmful lack of accuracy.

In this research, creep recovery experiments using a Parallel Plate Viscometer (PPV) are performed to quantify the magnitude of stress relaxation by extracting – through use of a Prony Series – the shear parameters for the glass material under test.

1.2 Research goals

The goal of this research is to extract the shear stress relaxation parameters of Pyrex® at a temperature near the glass transition region. The goal can be divided into four important points:

1) To understand how the Parallel Plate Viscometer instrument works and what happens during an experiment based on the observed temperature profile in the furnace and other external factors.
2) To extract from loading/unloading curves, the retardation curve from creep-recovery experiments.
3) To extract the retardation parameters from these data and to convert them into relaxation parameters with a Matlab program.
4) To compare the experimentally-realized results to those obtained using ABAQUS, a Finite Element Analysis (FEA) software.

1.3 Background on characterization of stress relaxation

For almost 50 years stress relaxation of glass has been studied by researchers and several theories had been established. The act of measuring the stress relaxation of glass is a difficult task and hence limited data exists in the literature for

multicomponent commercial glasses. One of the first experiments measuring stress relaxation was performed by Rekhson [2] with a relaxo-meter specifically designed to carry out stress behavior measurements. He showed mathematically that the stress relaxation of borosilicate glasses can be modeled using the Kohlrausch-Williams-Watt (KWW) function given by:

$$\Psi(t) = \exp[-(\frac{t}{\tau})^{\beta}]$$

where $\Psi(t)$ is the relaxation function, t is time, τ the relaxation time and β a constant. However, the main disadvantage of this function is its inaccuracy to describe multicomponent glasses and the relaxation of glass for the low times as it gives an infinite relaxation rate at time zero.

Duffrene *et al.* [3] proposed the generalized Maxwell model characterized by a Prony Series to describe the stress relaxation in glass.

$$\Psi(t) = \sum_{j=1}^{m} \omega_{ij} \exp(-\frac{t}{\tau_{ij}})$$

where $\Psi(t)$ is the relaxation function, ω_{ij} the relaxation weight and τ_{ij} the relaxation time. The advantages of using a Prony Series compared to the KWW function are (1) the Prony Series can be used to describe the retardation function as well as the relaxation function and (2) the generalized Maxwell model is easier to obtain the viscoelastic functions and constants.

1.4 Thesis Outline

This thesis is divided into seven chapters. Chapter 1 was dedicated to the introduction and the literature review. Chapter 2 explains in more details viscoelasticity and the mechanical properties of materials. Chapter 3 is dedicated to

glass science theory. Chapter 4 describes the experimental apparatus and the sample used. Chapter 5 presents the results of thermal analysis. Chapter 6 presents the experiments performed, the theoretical calculations done and an additional discussion of the results obtained. Chapter 7 concludes this thesis highlighting the key finding of the work and provides some recommendations for future work.

CHAPTER TWO

VISCOELASTICITY AND MECHANICAL PROPERTIES OF MATERIALS

2.1 Background on viscoelasticity

Viscoelasticity is a part of rheology; it is a science which studies the deformation and the flow of matter. Two extreme behaviors enable one to understand the properties of materials subject to viscoelasticity: the liquid which is governed by the laws of fluid mechanics discovered by Newton (*e.g.*, water has a 100% viscous behavior) and the solid which is governed by the solid state science laws with the theory of elasticity discovered by Hooke (*e.g.*, metal has 100% elastic behavior). Any behavior between these two extremes is referred to as being in a viscoelastic state.

Glasses have a viscoelastic behavior since the properties of these materials depend on temperature and time. Additionally, as glass properties vary widely with glass composition, viscoelastic properties vary significantly between simple glasses (*i.e.*, SiO_2) and commercial multicomponent glasses.

2.2 Background on glass science

2.2.1 Definitions

A glass is an amorphous solid completely lacking in long range, periodic atomic structure, and exhibiting a region of glass transformation behavior. More commonly, any material, inorganic, organic, or metallic, formed by any technique, which exhibits

glass transformation behavior can be considered a glass [4]. Different temperatures related to a specific range of viscosity enables the description of the glass transformation behavior:

- *Strain point*: temperature at which glass will relieve stresses over a period of hours. The viscosity reference is around $10^{13.5}$ Pa.s.
- *Annealing point*: temperature at which glass will relieve stresses (either compressive or tensile) in a matter of minutes. The range of viscosity is between 10^{12} to $10^{12.4}$ Pa.s.
- *Glass transformation temperature (T_g)*: temperature at which the material changes its behavior from being "glassy" (brittle) to being "rubbery" (elastic and flexible). The viscosity reference is around $10^{11.3}$ Pa.s.
- *Dilatometric softening point (T_d)*: temperature at which the sample reaches a maximum length in a length versus temperature curve during heating of a glass. Viscosity range: 10^8 to 10^9 Pa.s
- *Softening point*: temperature at which unsupported glass will begin to sag at a viscosity of $10^{6.6}$ Pa.s.
- *Working point*: temperature at which glass may be fully re-shaped. The glass may be formed into any shape and will sag completely under its own weight. The viscosity is around 10^3 Pa.s.
- *Melting temperature*: temperature at which the glass is fully liquid for a viscosity range from 1 to 10 Pa.s.

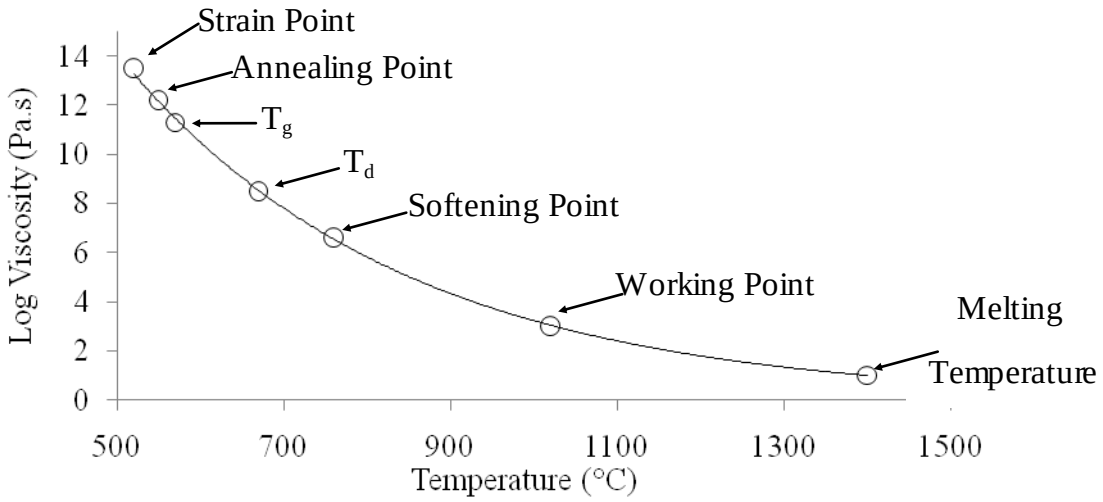

Figure 2.1. Typical curve for viscosity as a function of temperature with principal points

2.2.2 Principles of glass formation

Rapid cooling of the melt, a molten fusion of "batched" raw material components, to a temperature below the melting temperature enables the creation of a glass, if the cooling rate is high enough to avoid crystallization. Indeed, according to a material's Time-Temperature-Transformation (TTT) diagram (Figure 2.2), one can see that a critical cooling rate (CCR) exists which varies with glass composition. This temperature defines the minimum cooling rate required to yield a glass. Below the critical cooling rate one obtain a crystal or a glass with some fraction of crystals, above the CCR one can obtain a glass. This rate of cooling can be calculated with the slope of the curve taking with initial condition the melting temperature at time zero.

$$CCR = \frac{dT}{dt} \sim \frac{T_m - T_n}{t_n} \tag{2.1}$$

where T_m is the melting temperature, T_n is the temperature at the nose of the curve and t_n the time at the nose of the curve.

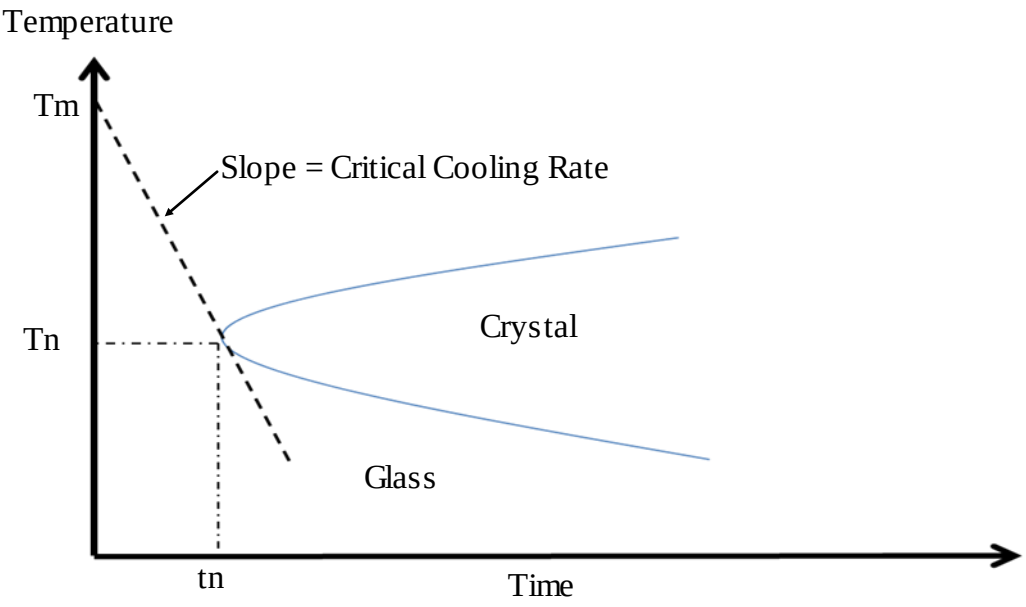

Figure 2.2. Typical curve for a Time-Temperature-Transformation diagram

Since glasses are cooled quickly, the viscosity increases rapidly limiting the rearrangement of atoms in the glass structure preventing the ordering of a periodic structure seen in crystals. The resulting glass is not in thermodynamic equilibrium and its formation is governed by the laws of kinetics. The Volume/Temperature diagram illustrates this non-equilibrium system for glasses compared to crystalline matter. At high temperature, the volume occupied by the melt is high and starts to decrease as the temperature decreases below this point. In the case where cooling occurs at a rate lower than CCR, we have formation of a crystal, and the enthalpy changes dramatically; this is not the case for a glass quenched at a rate above the CCR. However, if we have formation of a glass, we obtain a supercooled liquid. The glass

obtained at room temperature keeps in memory the "path" it took to be created, which explains why the same glass can have different T_g values.

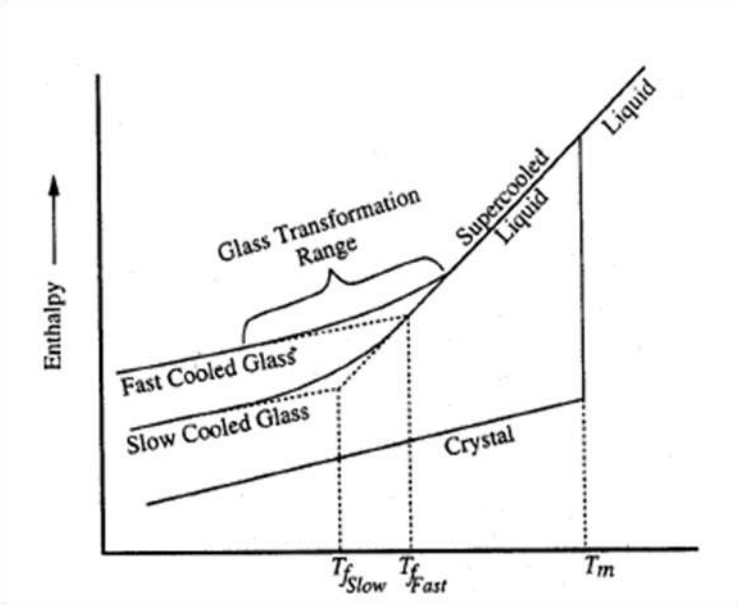

Figure 2.3. Enthalpy/Temperature diagram for a glass and a crystal [4]

2.3 Phenomenological models in linear viscoelasticity

Five parameters are defined to describe the linear viscoelasticity of materials: the stress σ, the strain ε, the rate of strain $d\varepsilon/dt$, the shear modulus G and the viscosity η. The models are built with two primary mechanical geometries shown in Figure 2.4: a spring and a dashpot.

The spring, which provides a linear relationship between the applied force and the resulting displacement, models a material's elastic behavior. The dashpot, with a linear relationship between the force and the rate of displacement, can be use to model the viscous behavior.

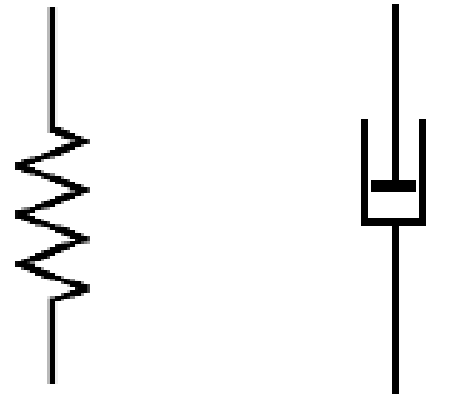

Figure 2.4. Primaries elements for viscoelastic models

2.3.1 The Maxwell model

The Maxwell model for viscoelastic materials combines a spring and a dashpot in series. The stresses in the spring and in the dashpot are the same and the total strain is the sum of the spring strain and the dashpot strain.

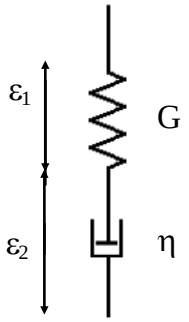

Figure 2.5. Maxwell model

For the spring part

$$\sigma = G\varepsilon_1 \qquad (2.2)$$

For the dashpot part

$$\sigma = \eta \frac{d\varepsilon_2}{dt} \tag{2.3}$$

The total strain is:

$$\varepsilon = \varepsilon_1 + \varepsilon_2 \tag{2.4}$$

(1) If we combine (2.2), (2.3) and (2.4) we obtain the following differential equation:

$$\dot{\varepsilon} = \frac{\dot{\sigma}}{G} + \frac{\sigma}{\eta} \tag{2.5}$$

(2) The following equation describes the stress relaxation:

$$\tau(t) = \tau(0) exp^{\frac{-t}{\lambda}} \tag{2.6}$$

Where λ is the relaxation time: $\lambda = \frac{\eta}{G}$

Other phenomenological models exist such as the Kelvin-Voigt model (one spring and one dashpot in parallel), the Zener model (a Kelvin-Voigt model in series with a spring), the Burgers model (a Kelvin-Voigt model in series with a spring and a dashpot). However, none of these models is sufficient to correctly characterize the viscoelastic behavior of glass since they don't model well enough the stress relaxation behavior for all times, thus a more complex model, such as the generalized Maxwell model, is necessary.

2.3.2 The generalized Maxwell model

The generalized Maxwell model includes several Maxwell elements in parallel; as shown in Figure 2.6. Each Maxwell element represents the relaxation of one type of bound. That's why in theory, glasses need several Maxwell elements since the angle among the atoms are different and a crystal should have only one element.

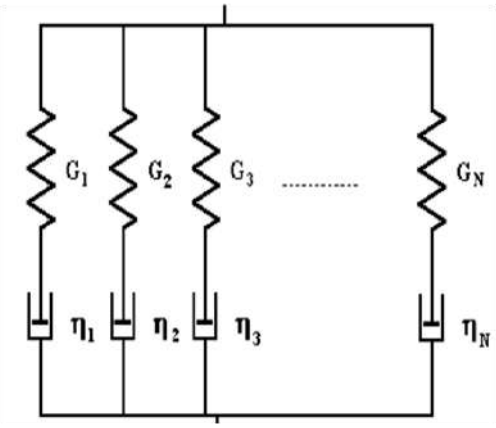

Figure 2.6. generalized Maxwell model

The generalized Maxwell model can be represented by solving a Prony Series equation of the form:

$$\Phi_i(t) = \sum_{j=1}^{m} v_{ij} exp^{\frac{-t}{\lambda_{ij}}} \tag{2.7}$$

where $\Phi_i(t)$ is the retardation function, the index i = 1,2,u refers to the shear behavior (i=1), hydrostatic (i=2) and uniaxial (i=u), v_{ij} and λ_{ij} are the retardation weights and times respectively and m is the number of terms in the Prony Series, which corresponds to the number of Maxwell elements.

2.4 Dynamic resonance method

This method enables the definition of some parameters such as the modulus and the viscosity. During these experiments, the material is subjected to a sine wave strain as shown by the equation 2.8.

$$\varepsilon(t) = \varepsilon_0 \cos(\omega t) \tag{2.8}$$

The stress measured is a sine wave with the same frequency but with a different phase compared to the strain for a viscoelastic material.

$$\sigma = \sigma_0 \cos(\omega t + \delta) \tag{2.9}$$

where δ is called the loss angle.

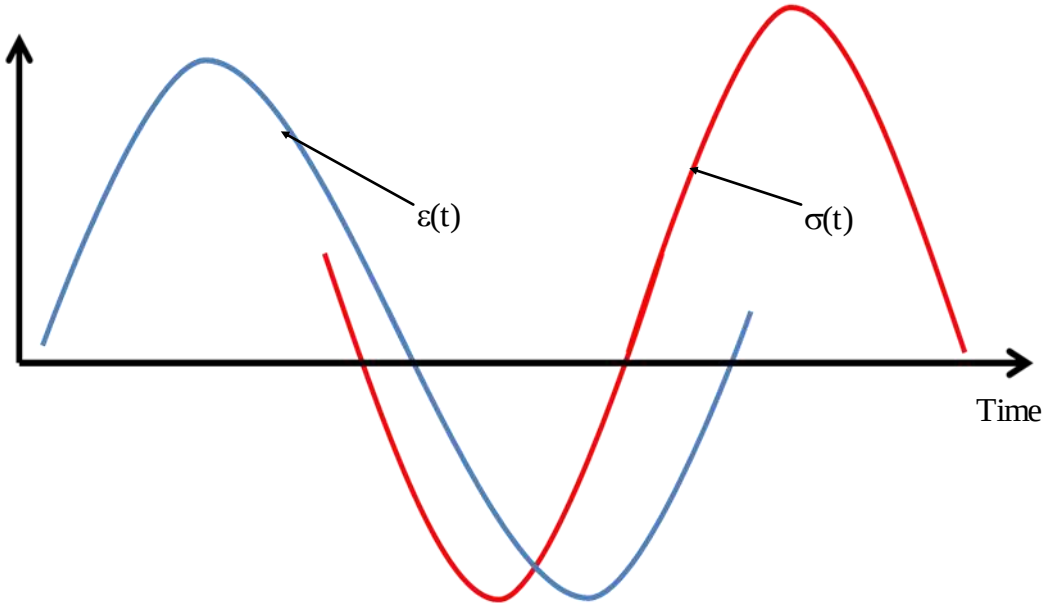

Figure 2.7. Stress and strain during an experiment by dynamic resonance method

Moreover, we can define the stress as a sum of two different contributions : with on the one hand a part which defines the elastic solid with the Hooke's law and

on the other hand a part which defines the viscous solid with the Newtonian's law. According to Equation 2.9, the stress can be calculated by:

$$\sigma(t) = \sigma_0 \cos(\omega t + \delta) \tag{2.10}$$

Which can be explained:

$$\sigma(t) = \sigma_0 \cos(\delta) cos(\omega t) - \sigma_0 \sin(\delta) cos(\omega t + \frac{\pi}{2}) \tag{2.11}$$

To result in:

$$\sigma(t) = \underbrace{\left[\frac{\sigma_0}{\varepsilon_0}\cos(\delta)\right]}_{\text{Elastic modulus G'}} \underbrace{\varepsilon_0 \cos(\omega t)}_{\text{Hooke's solid}} + \underbrace{\left[\frac{\sigma_0}{\varepsilon_0}\sin(\delta)\right]}_{\text{Loss modulus G"}} \underbrace{\varepsilon_0 \cos(\omega t + \frac{\pi}{2})}_{\text{Newtonian liquid}} \tag{2.12}$$

where the dynamic moduli G' and G" are defined by the following equations in the range of linear viscoelasticity, *i.e.*, for small deformations.

$$G'(\omega) = \lim_{\varepsilon_0 \to 0} \frac{\upsilon_0}{\varepsilon_0} \cos(\delta)$$
$$G''(\omega) = \lim_{\varepsilon_0 \to 0} \frac{\sigma_0}{\varepsilon_0} \sin(\delta) \tag{2.13}$$

Furthermore, instead of applying a sine wave strain we can do the same experiment with an applied sine wave stress and calculate the strain and the associated dynamic moduli J' and J" .

$$\sigma = \sigma_0 \cos(\omega t) \tag{2.14}$$

$$\varepsilon(t) = \left[\frac{\varepsilon_0}{\sigma_0}\cos(\delta)\right]\sigma_0\cos(\omega t) + \left[\frac{\varepsilon_0}{\sigma_0}\sin(\delta)\right]\sigma_0\cos(\omega t + \frac{\pi}{2}) \tag{2.15}$$

$$J'(\omega) = \lim_{\varepsilon_0 \to 0} \frac{\varepsilon_0}{\sigma_0}\cos(\delta) \tag{2.16}$$

$$J'' = (\omega) = \lim_{\varepsilon_0 \to 0} \frac{\varepsilon_0}{\sigma_0}\sin(\delta) \tag{2.17}$$

2.5 Stress relaxation

For viscoelastic materials in the transition region, the relationship between stress and strain involves time and depends on how load is applied to the material. In the stress relaxation experiment, the stress σ is measured as a function of time after applying a constant strain ε_0 on the material. Depending on the temperature one of two responses can be observed as illustrated in Figure 2.8

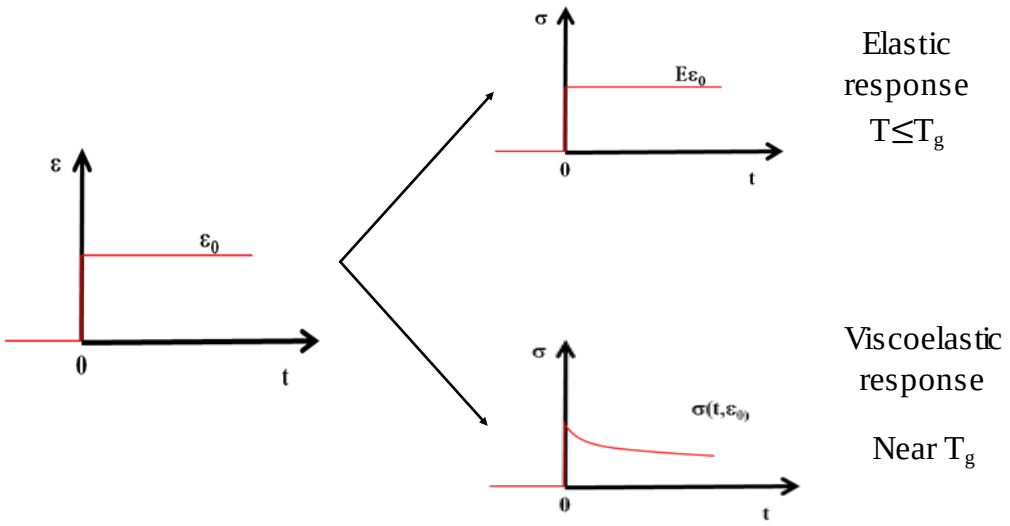

Figure 2.8. Stress relaxation experiment

For an elastic body, the stress at t > 0 is only function of the strain.

$$\sigma(t,\varepsilon_0) = \sigma(\varepsilon_0) = \begin{cases} E(\varepsilon_0)\varepsilon_0 & \text{Non linear elastic body} \\ E\varepsilon_0 & \text{Linear elastic body} \end{cases} \quad (2.18)$$

For a viscoelastic body, the stress is a function of deformation but also time.

$$\sigma(t,\varepsilon_0) = \begin{cases} E(\varepsilon_0,t)\varepsilon_0 & \text{Non linear viscoelastic body} \\ E(t)\varepsilon_0 & \text{Linear viscoelastic body} \end{cases} \quad (2.19)$$

2.6 Creepexperiment

In a creep experiment, a constant stress σ_0 is applied to the materials and the strain ε is measured. Again, the observed material response depends on the temperature at which the test is carried out as shown in Figure 2.9.

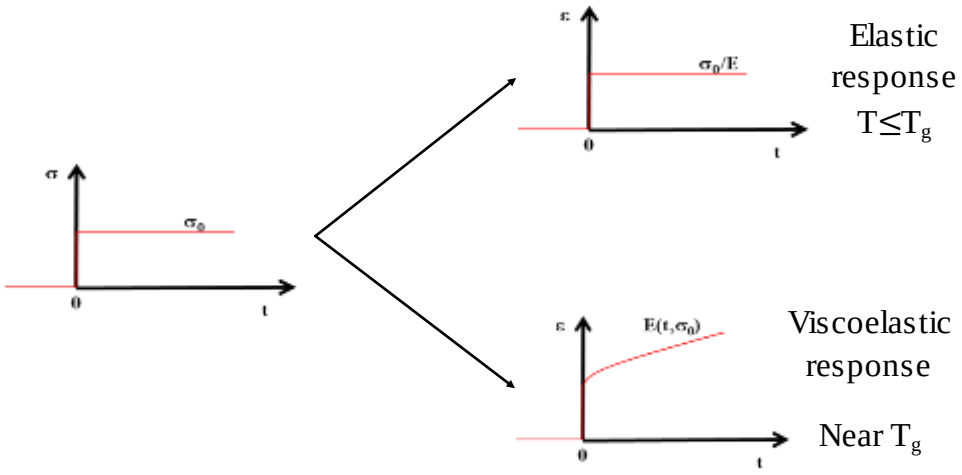

Figure 2.9. Creep experiment

Creep-recovery experiment

A creep-recovery experiment consists of applying a constant stress to the material and the instantaneous removal of the load at a given time, t. As soon as the load is removed, the material starts recovering towards it's original unloaded shape as shown in Figure 2.10 where three principal zones in a displacement versus time plot, can be identified:

Zone 1 corresponds to the elastic response of the material. The amplitude of the elastic response due to the applied stress (segment [AB]) and removal (segment [CD]) should be equal.

Zone 2 is the delayed strain part (line (DE)), where the glass deforms slowly. The generalized Maxwell model models this relaxation using a Prony Series.

Zone 3 is the steady-state where the glass does not relax anymore.

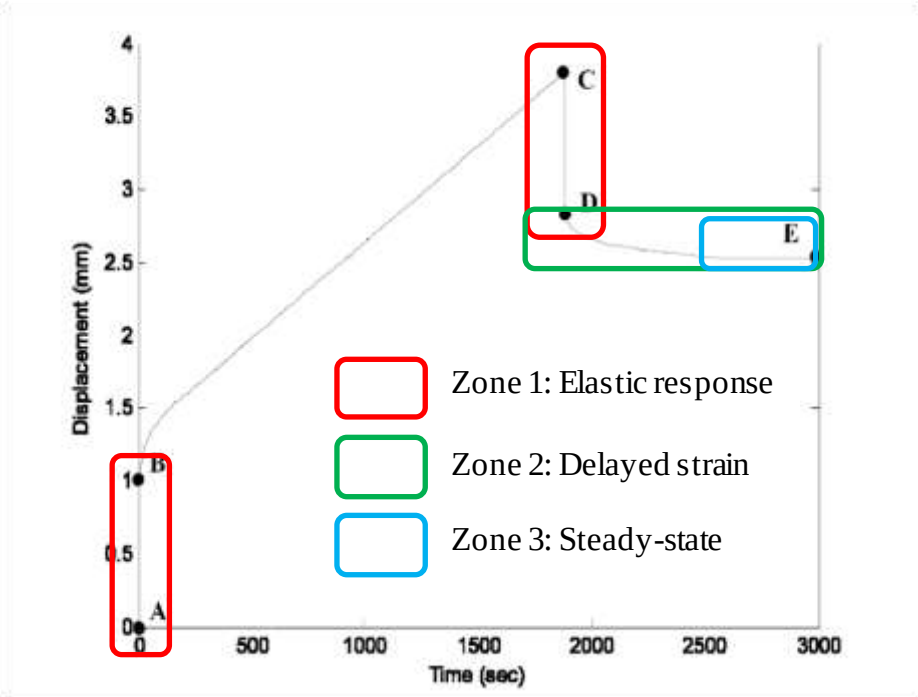

Figure 2.10. Theoretical curve for a stress relaxation experiment [5]

2.7 Thermo-rheological simplicity between time and temperature

The thermo-rheological simplicity between time and temperature enables the prediction of how temperature affects the viscoelastic parameters such as the viscosity and the shear modulus. For example, we can consider a recovery experiment at two different temperatures T_1 and T_2 such that $T_1<T_2$. The glass at the higher temperature will have a faster recovery. Therefore, going from temperature T_1 to temperature T_2 is equivalent to multiplying the time scale by a constant factor $a_{T_1 \to T_2}$, where $a_{T_1 \to T_2}$ is called shift factor, is related to material viscosity at temperature and can be calculated with the following formula:

$$a_{T_1 \to T_2} = \frac{\eta_0(T_1)}{\eta_0(T_2)} \tag{2.20}$$

here $\eta_0(T_1)$ and $\eta_0(T_2)$ are the viscosity for the material at temperature T_1 and T_2, respectively.

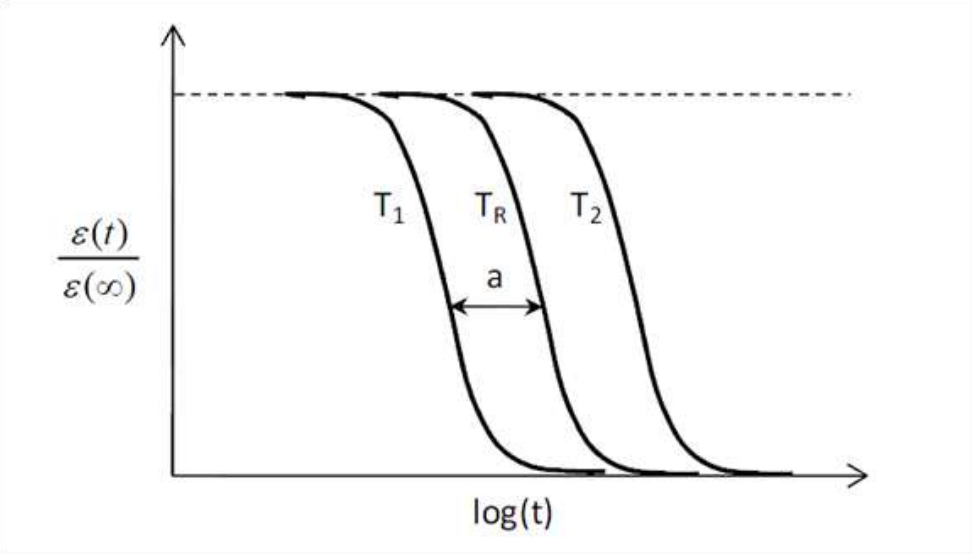

Figure 2.11. Thermo-rheological simplicity between time and temperature [6]

2.8 Mechanical properties of materials

2.8.1 Tension test

A tension test is an experiment which enables the measurement of the resistance of the material to an applied tensile stress. Most of materials can be described by one of two different cases:

In a ductile material, the initial deformation is elastic. The strain-stress curve is a straight line and the slope value provides Young's modulus E. After the elastic region, the curve starts to level off, which corresponds to the region of plastic deformation. The curve then reaches a maximum which determines the ultimate yield stress. From this point, the cross-section of the area of the specimen decreases and the material fails.

In a brittle material, the material fails just after the elastic region. These two cases are illustrated in Figure 2.12.

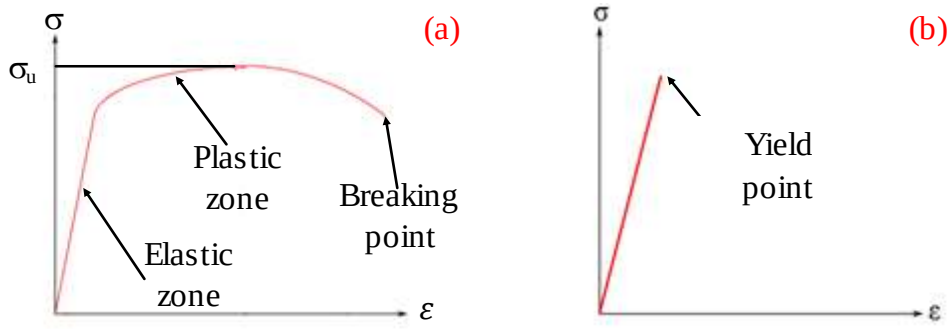

Figure 2.12. Typical curve during a tension test for a) a ductile material and b) a brittle material

2.8.2 Compression test

A compression test is an experiment which enables measurement of the resistance of a material to compressive stress. We can study two different cases:

In a ductile material, the material will deform plastically and will either fail by crushing or compress with very large deformation.

In a brittle material, we obtain the same curve $\sigma=f(\varepsilon)$ shown previously for a brittle material in tension but with negatives stress and strain.

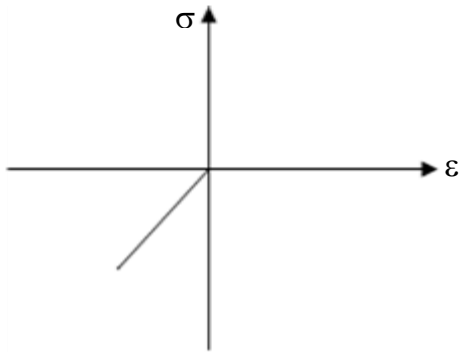

Figure 2.13. Typical curve during a compression test for a brittle material

2.8.3 Hydrostatic stress

Consider a cube shown in Figure 2.14 where we apply three normal stresses of equal magnitude and in the three space directions. In the case of hydrostatic forces, the cube will deform uniformly in the space: $\sigma_{11} = \sigma_{22} = \sigma_{33}$, resulting in a change in sample volume.

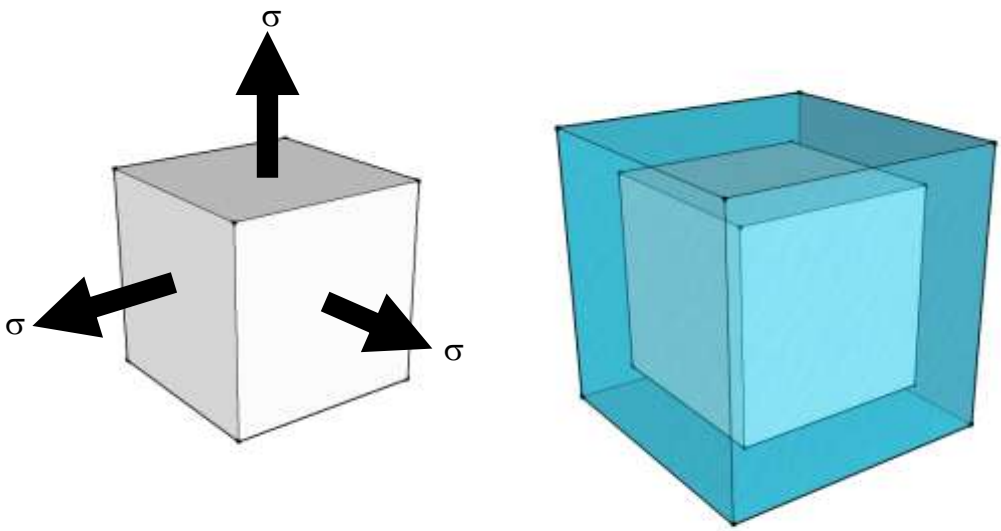

Figure 2.14. Cube before (on left) and after (on right) the application of a hydrostatic force

2.8.4 Shear stress

A shear stress is defined as a stress which is applied parallel or tangential to a face of a material, as opposed to normal stress which is applied perpendicularly. Let us consider a square under shear stress shown in Figure 2.15.

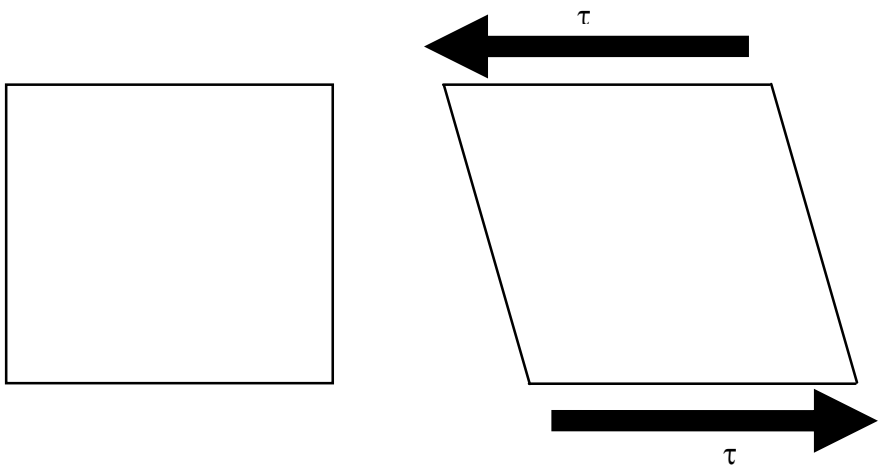

Figure 2.15. Square before (left) and after (right) the application of a shear force

The average stress can be calculated with the following formula:

$$\tau = \frac{V}{A} \tag{2.21}$$

where τ is the shear stress applied (Pa), V the transversal force applied (N) and A the cross sectional area (m^2)

Study case: A spring (pure shear experiment)

The shear stress developed through the coil cross-section includes a large torsional shear component and a small transversal shear component. [5].

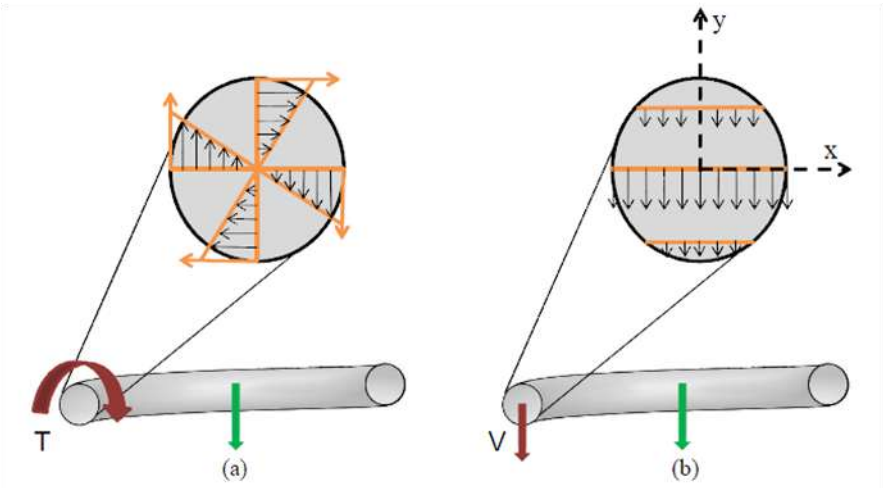

Figure 2.16. Stress distributions inside spring coil (a) torsional stress (b) transversal stress

The torsional stress is given by the formula [7]:

$$\tau_T = \frac{T\rho}{J} \tag{2.22}$$

where T is the torque (N.m), ρ is the distance from the center of the cross-section to the point of interest (m) and J is the polar moment of inertia (m^4) and given by:

$$J = \frac{\pi D^4}{32}$$

The transversal stress is given by:

$$\tau_V(x, y) = \frac{VQ}{It} \tag{2.23}$$

where V is the total shear force (N), Q is the partial first moment of the cross-sectional area above the point of interest, t is the thickness of the material (m) perpendicular to the shear at the point of interest and I the moment of inertia of the cross-section. For a cylinder cross-section I is equal to: $I = \frac{\pi D^4}{64}$.

2.8.5 Instantaneous elastic response of a spring

The elastic response of a spring under compression, which is necessary to extract the shear parameter (see chapter 6), is given by the Equation (2.24) [8]

$$\delta_i = \frac{8FD^3N}{d^4G}\left(1 + \frac{1}{2\left(D/d\right)^2}\right) \tag{2.24}$$

where δ_i is the elastic response (m), F is the force applied (N), N is the number of active coil, G is the shear modulus of the material (Pa), D is the pitch diameter of the spring (m) and d is the coil diameter of the spring (m).

CHAPTER THREE

GLASS SCIENCE THEORY

As explained in Chapter 2, glasses are amorphous materials with no long range atomic order and exhibit glass transformation behavior with a glass transition temperature T_g. Moreover, in order to create a glass, an adequate cooling rate between the liquidus and the solidus temperatures must be maintained to prevent the formation of crystalline structures. Moreover, several parameters are needed to describe the stress relaxation of glasses due to the fact that the bond angles among the atoms are not the same and thus, upon heating to a temperature near T_g will relax differently.

3.1 Structural theories of glass formation

3.1.1 History

Goldschmidt [4] discovered that glasses with a general formula R_nO_m form most easily when the ionic radius ratio R and the oxygen O is between 0.2 and 0.4. This ratio tends to produce cations surrounded by four oxygen atoms in a tetrahedral. A few years later, Zachariasan [4] established that a vitreous network is necessary for glass formation in the oxide glass system. He proposed that a network is composed of tetrahedrals connected at all four corners and triangles but is not periodic and symmetric like a crystal. From these observations, he summarized three statements:

1) The ratio of cations in the material is high and surrounded with oxygen in tetrahedral or triangle geometries. This ratio has to be high in order to make a continuous network.

2) The tetrahedrals and triangles are only connected by their corners.

3) Some oxygens are only linked to only two cations.

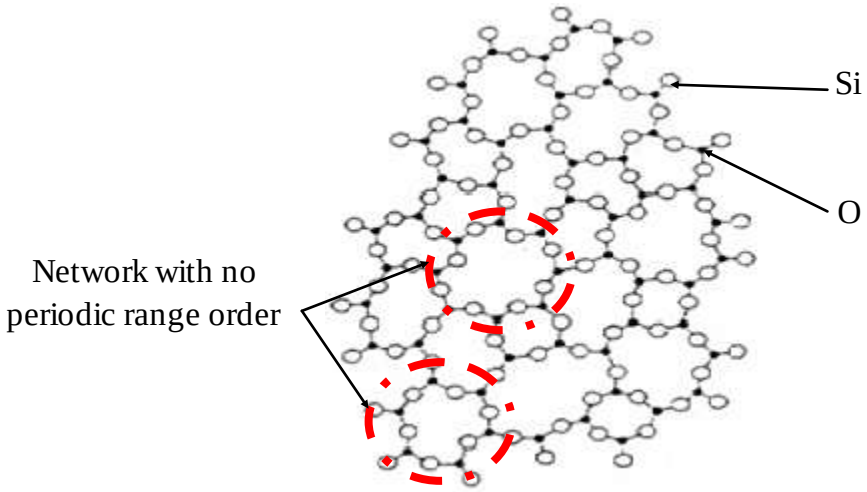

Figure 3.1. Schematic of silica glass (SiO_2)

Other scientists tried to establish other theories on glass formation such as Smekal [4] who said that melts most likely to form a glass is compounded with intermediate bonds which are partially ionic (if it was too ionic there would be no directionality and then no network) and partially covalent (if it was too covalent the network would be too rigid). Later, Stanworth [4] classified oxides glasses into three different groups based on the electronegativity of the cation:

- Group I "*Network formers*": Cations which form bonds with oxygen with a fractional ionic character near 50%. These cations produce the best glasses.

- Group II "*Intermediates*": These cations are not enabled to form a glass by themselves due to their lower electronegativity (more ionic bonds) but they can replace partially some cations of the Group I.
- Group III "*Modifiers*": Cations with very low electronegativity and which forms ionic bonds. They are used to modify the network of the structure.

3.1.2 Kinetics and thermodynamics of glass formation

As discussed earlier when we cool a liquid below its melting point the thermodynamics predict crystal formation unless the materials is cooled fast enough to avoid crystallization and to form a glass. Thus, to avoid crystallization, the following two required steps (i) the nucleation step and (ii) the crystal growth step, must also be avoided.

Nucleation: It is compulsory to obtain nuclei in order to observe crystal growth. The nuclei can occur homogeneously, *i.e.* they are directly formed in the melt or heterogeneously, *i.e.* a dust or the crucible wall is enough to start the reaction of formation of nucleus. This reaction occurs only if the thermodynamics and the kinetics barriers are activated. The thermodynamic barrier involves that the free energy in the melt changes when a nucleus is formed. The kinetics barrier involves that the nuclei formed can move into the melt to allow the growth of crystal. This process is governed:

$$I = A\exp\left[-\left(\frac{W^* + \Delta G_D}{kT}\right)\right] \quad (3.1)$$

where A is the pre-exponential factor, W* and ΔG_D are the thermodynamics and kinetics barrier (J), k is the Boltzmann constant ($J.K^{-1}$) and T is the temperature (K).

During the formation of a nucleus the volume free energy of the system decreases and the surface free energy increases due to the creation of an interface between the nucleus and the melt. Equation (3.2) gives the thermodynamics barrier.

$$W = \frac{4}{3}\pi r^3 \Delta G_v + 4\pi r^2 \Upsilon \tag{3.2}$$

where ΔG_V is the change in volume free energy (J) and Υ is the surface energy ($J.m^{-2}$) of the interface nucleus/melt.

The thermodynamic energy needed to activate the nucleus barrier is given by:

$$W^* = \frac{16\pi\Upsilon^3}{3\Delta G_V^2} \tag{3.3}$$

Grain growth: Growth of crystals can only occurs if the melt includes nuclei with a radius r > r*; where r* is the critical radius of nuclei for growth. Using the same thermodynamics and kinetics considerations shown previously. Equation (3.4) gives the crystal growth rate.

$$U = a_0 \nu \exp\left(-\frac{\Delta_E}{kT}\right)\left[1 - \exp\left(\frac{\Delta_G}{kT}\right)\right] \tag{3.4}$$

where a_0 is the interatomic separation distance (m), ν is the vibrational frequency (Hz), ΔE and ΔG are respectively the kinetic and thermodynamic barrier (J).

3.2 Glass melting

3.2.1 Materials used

Different ways exist to form a glass (Sol-gel techniques, physical vapor deposition etc …) but the most common is to melt the raw components together to form a melt,

and then to quench to a glassy state. Five categories of raw materials can be used to form a glass: the glassformers, the flux, the property modifier, an optional colorant and the fining agent. Furthermore, the material can be further defined depending on which type of glass we want to create.

- The glassformers are the materials which are used to create the network of the glass, *e.g.* the silica SiO_2 for silica glasses, telluric oxide TeO_2 for tellurite glasses.
- Flux materials are added to the melt is order to decrease the melting temperature of the glassformer. Indeed, most glasses require high temperature to melt which is very expansive in industry; *e.g.* if soda (NaO) is added to silica, the temperature is reduced from 2000°C to 1600°C. The cations Na^+ are relatively big and they tend to break the Si-O-Si bonds. The network structure is less rigid and the melting temperature decreases. Unfortunately, adding flux materials result in a loss of glass properties specially the chemical durability.
- The property modifiers are added to counteract the effects of flux materials. They have to be added in very precise quantity in order to obtain the desired composition and results for the glass properties.
- Colorants are added only to give a color to the glass. Very often 3d and 4d transition metals are used to color the material. Indeed, according to their oxidation state these metals are able to have different colors. Other species as gold particles or iron oxides may be used.
- The fining agents are materials added to remove bubbles from the melt and then the final glass (*e.g.*, NaF, Na_3AlF_6…)

3.2.2 Forming glasses

Forming glasses involves fours steps. The first step is to mix the raw components together in a way that decreases the average grain size, improves homogeneity of the batch and then the homogeneity of the melt. During the second step the batch is melted at a temperature T during a time t. Third step is the quenching step where the glass is cooled quickly outside the oven. During quenching, the glass is under high stresses due to the thermal gradient between the outside of the glass (cooler) and the glass core (warmer). These stresses could be harmful and result in a break. Therefore, the fourth step called the annealing step is necessary. During the annealing process, the glass is put at a temperature of 40°C below T_g for a few hours to relax the stresses.

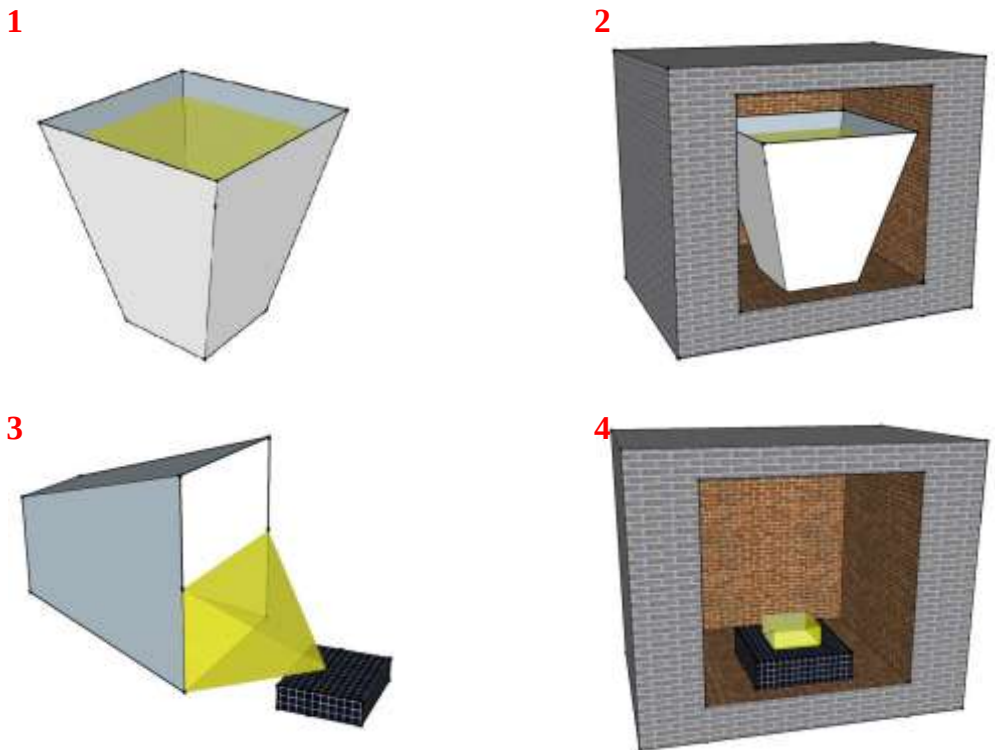

Figure 3.2. The four steps to create a glass: 1) Batch with raw materials, 2) Melting process, 3) Quenching, 4) Annealing

3.3 Types of glass

Many types of glass exist. However, we have focused on three different types in this thesis: Pyrex®, NBK7® and L-BAL35®.

3.3.1 Pyrex® glass

Pyrex® is one of the most well known glasses in the world due to its many applications, such as in cooking plates, laboratory glassware, and telescopes. Pyrex® was invented at the beginning of the twentieth century by the Corning Company. They created a borosilicate glass with a very low thermal expansion coefficient, resisting to thermal shock and chemical attack. It's nominal composition in shown in Table 3.1 [9]

Table 3.1. Nominal composition of Pyrex® glass

Name	Nomenclature	Composition (mol %)
Silica	SiO_2	80
Boric acid	B_2O_3	13
Aluminum oxide	Al_2O_3	2.25
Iron III oxide	Fe_2O_3	0.05
Sodium hydroxide	NaOH	3.5
Potassium hydroxide	KOH	1.1

Table 3.2 summarizes the physical and thermo-mechanical properties of Pyrex®.

Table 3.2. Properties of Pyrex® [9]

Young's modulus (GPa)	65.8
Absolute density (g.cm^{-3})	2.23
Compression resistance at 20°C (bars)	3600
Tensile resistance at 20°C (bars)	142
Poisson's ratio	0.2
Thermal expansion coefficient (°C^{-1})	32.5 10^{-7}
Glassy temperature (°C)	~560

In this thesis we decided to work first with Pyrex® due to its availability in many shapes and sizes as well as its malleability and resistance to the thermal shock encountered during sample manufacturing.

3.3.2 N-BK7® glass

N-BK7® glass is another common borosilicate glasses, used primarily in optical applications in the frequency range between visible and infra-red from 350nm to 2000nm. This glass is derived from the BK-7® glass composition, and the "N" denotes it has been produced without toxic elements such as arsenic. Moreover, while the optical properties may be the same between these two glasses (*i.e.*, index of dispersion) the thermal and rheological parameters can vary largely [10]. Its huge transmission range makes it a very good candidate for optical utilization as shown in Figure 3.3.

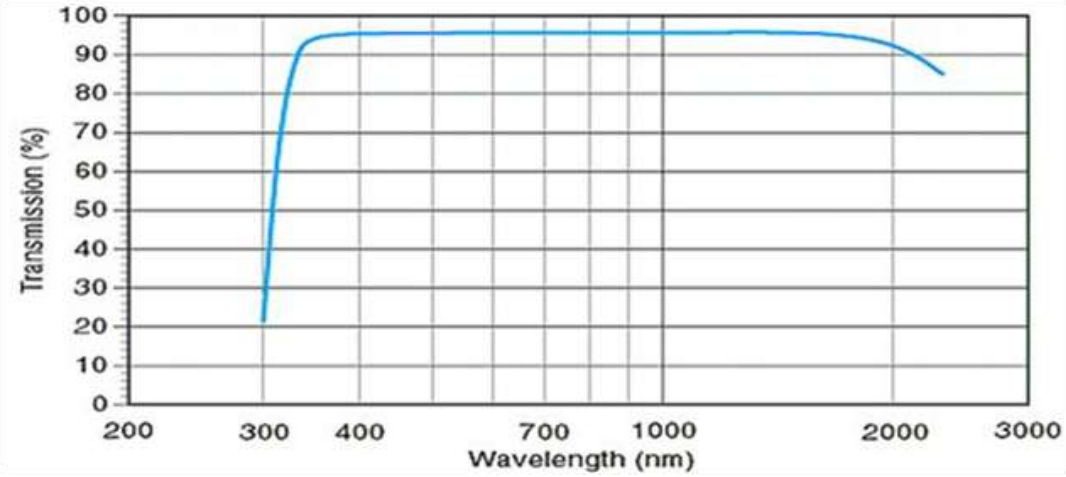

Figure 3.3. Transmission curve for BK-7® and for N-BK7® glasses [11]

Table 3.3 summarizes some thermal and mechanical properties for BK-7® and N-BK7®.

Table 3.3. Thermal and mechanical properties of BK-7® and N-BK7®[12][13]

Properties	**BK-7®**	**N-BK7®**
Coefficient of thermal expansion ($^{\circ}C^{-1}$)	$8.3\ 10^{-6}$	$8.3\ 10^{-6}$
Absolute density ($g.cm^{-3}$)	2.51	2.51
Glass transition temperature ($^{\circ}C$)	557	560
Refractive index n_d	1.51680	1.51680

3.3.3 L-BAL35® glass

L-BAL35® is a silicate-based glass and, like N-BK7®, has good optical properties and is widely used in optical components. The advantage of this glass is its refractive index(1.58913) [14] which is close to the refractive index of N-BK7®. This coefficient is related of the speed of light inside the material.

Unfortunately, the main disadvantages of these glasses (L-BAL35® and N-BK7®) are that they are very sensitive to thermal shock; they can crystallize quickly when they are heated and held near T_g [5], and they easily form bubbles during the sample manufacturing without proper care.

CHAPTER FOUR

EXPERIMENTAL SETUP

4.1 Parallel Plate Viscometer and sample used

The Parallel Plate Viscometer (PPV) Model PPV-1000 used for the experiments in this study is manufactured by the Orton Ceramic Foundation. The Parallel Plate Viscometer is generally used to measure the viscosity of solid glass cylinders (*i.e.*, usual size is 5mm height) in the viscosity range of $\log_{10}(\eta)$=6.0 to $\log_{10}(\eta)$=3.0 Pa.s as a function of temperature up to 1000°C based on ASTM standard number C-1351M. As shown in Figure 4.1, the machine includes a cylindrical heating coil that forms the furnace chamber which is capped at both ends by two Inconel disks. The furnace temperature is measured by a type "S" thermocouple connected to the temperature controller. The original system includes a LVDT (Linear Variable Differential Transformer) to measure vertical displacement.

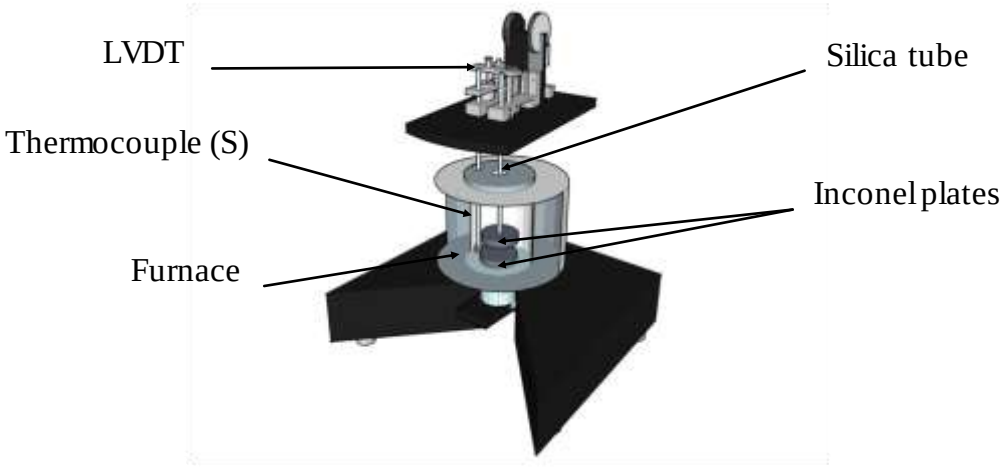

Figure 4.1. Schematic of a Parallel Plate Viscometer

The experimental protocol for measuring viscosity includes the following steps. A cylindrical glass sample is polished to obtain flat and parallel ends. The glass sample is placed between the top and bottom Inconel plates (*i.e.*, 44 millimeter diameter by 6 millimeter thick disks of a refractory metal alloy Inconel). In order to prevent the glass sample from sticking to the Inconel disks, two thin sheets of platinum or aluminum foils are inserted between the sample surface and the two plates. A motorized system closes the furnace by raising the heating coil. A counterbalancing pulley system is used to apply a vertical compressive force on the sample by adding a weight on top of silica rod directly above the sample. The operator can enter as input data the diameter, the length of the sample, the rise and the temperature in the furnace or the weight of the load. The sample is then heated to the desired temperature. After the steady state temperature reached, a weight is added which initiates the viscosity test. During the compression, the displacement is measured by the LVDT which provides a voltage. The software converts this voltage into a displacement and then into a viscosity according to the formula:

$$\eta = 2\pi \frac{Mgl^5}{30V\left(\frac{dl}{dt}\right)(2\pi l^3 + V)} \tag{4.1}$$

where η is the viscosity (Pa.s), M the load applied (g), g is the acceleration of gravity (980 cm.s^{-2}), l (cm) is the specimen thickness at time t (s) and V is the specimen volume (cm^3).

In the tests for the present study, spring samples of approximately 50mm height are used as shown is Figure 4.2. The spring also presents the following characteristics with a pitch diameter of 28.7mm and four active coils of diameter 5.13mm.

Figure 4.2. Spring sample used for creep-recovery experiment in the Parallel Plate Viscometer

4.2 Linear Variable Differential Transformer (LVDT)

4.2.1 Description

This device enables to measure a linear displacement without friction. As illustrated in Figure 4.3, it is composed of a transformer (with two solenoids) and a ferromagnetic core. This core moves along the direction of the cylinder and modifies the magnetic field of the transformer. This magnetic field variation is converted into a voltage which is then converted into a displacement. The main advantage of the LVDT is that there is no contact and therefore no friction between the core and the solenoids, which provides very high sensitivity.

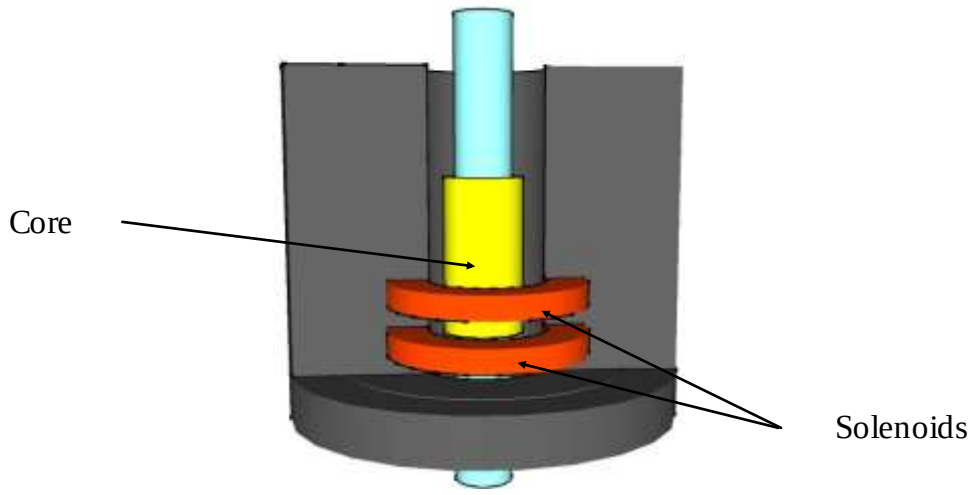

Figure 4.3. Schematic of a LVDT (partial cut through exterior tube)

The sampling rate of the original PPV data acquisition system is one data point of every 5 seconds, which is sufficient for viscosity measurements but insufficient for creep-recovery experiments. Therefore, the LVDT was diverted and connected to a data acquisition system with a sampling rate of 100 points per second. The LVDT was

connected to a signal conditioner "Schaevitz sensors ATA 2001". The signal conditioner was connected to an InstruNet World Model 100 data box which transforms the LVDT magnetic signal into an electrical voltage. The data box is then connected to a computer to visualize the signal.

Figures 4.4 and 4.5 summarize the electrical connections before and after the addition of the databox.

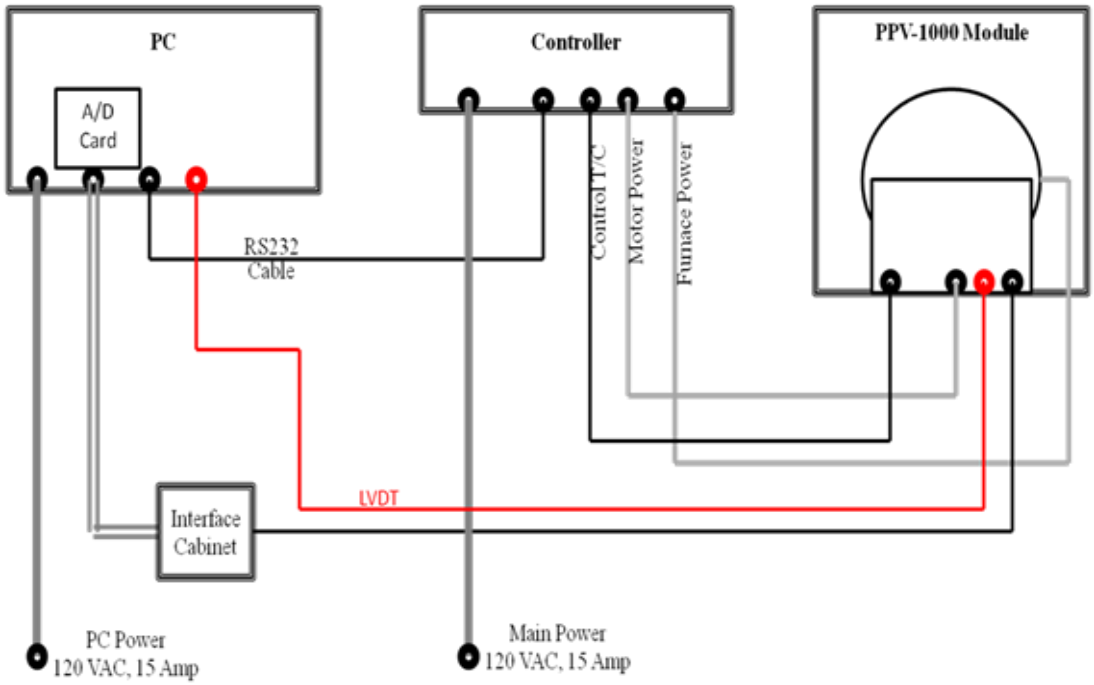

Figure 4.4 Electrical connections before the addition of the data box

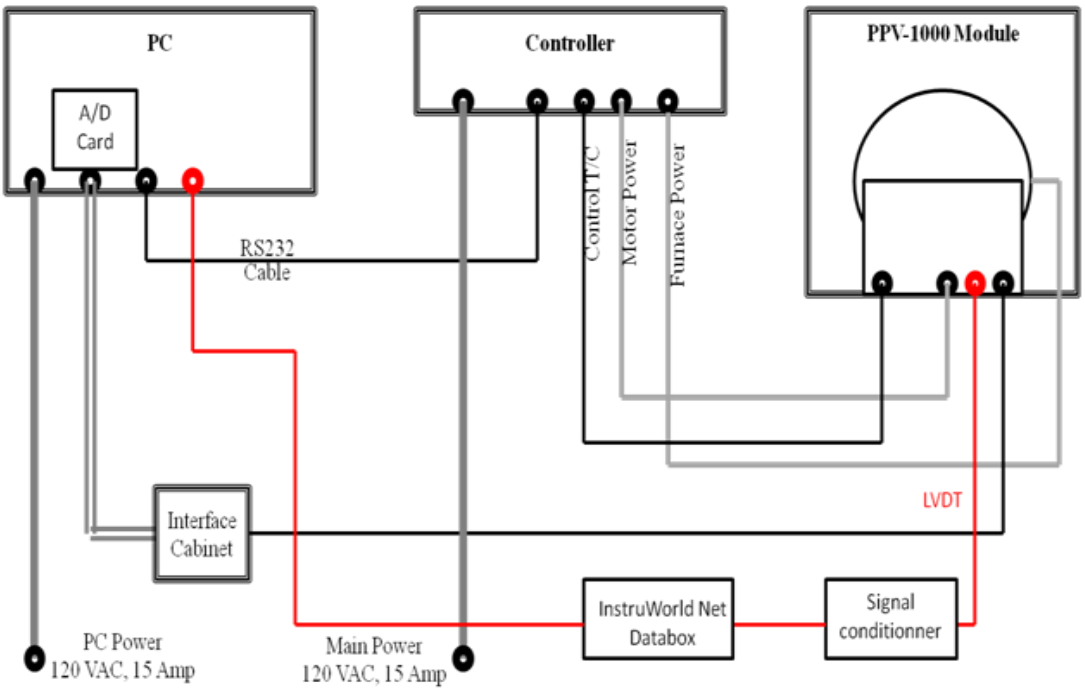

Figure 4.5. Electrical connection after the addition of the data box

4.2.2 LVDT calibration

The LVDT was calibrated and checked for linearity. This was done by increasing the height of the LVDT with thin glass layers of known thickness. The curve voltage (V) as a function of height (mm) in the range of +/- 5V, shown in Figure 4.6, demonstrates the linearity of device. It will be now easier for the next PPV experiments to convert the voltage into a displacement.

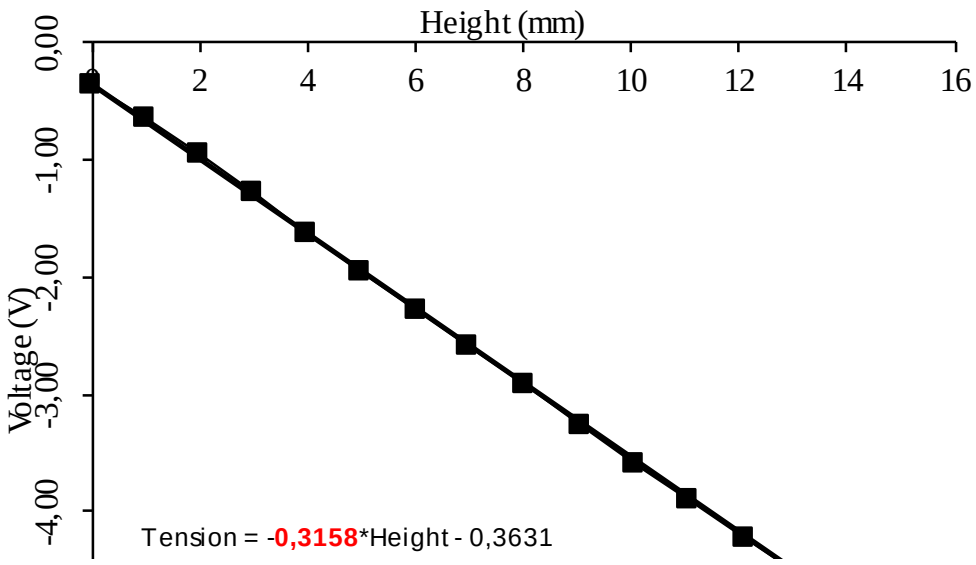

Figure 4.6. LVDT calibration Voltage = f (Height)

CHAPTER FIVE

THERMAL ANALYSIS

Before starting the experiments it is important to check the temperature homogeneity inside the furnace. As stated in Chapter 4, the size of the spring used here (*i.e.*, 50mm height) is much larger than the size of the usual sample (*i.e.*, 5mm height) in the PPV's normal use. The goals of the following experiments were (i) to determine the temperature homogeneity as a function of height at the center and near the furnace walls, and (ii) to measure the effect of the presence of a sample on the temperature profile.

5.1 Temperature near the furnace walls and at the center without sample

Verifying the temperature homogeneity inside the furnace is important in order to know if the whole sample is at the same temperature or not since temperature can affect significantly the viscoelastic properties of glass. The vertical position of the thermocouple is increased step-by-step with increments of one millimeter. The experiment was performed three times for repeatability and to determine a correct standard deviation for the data.

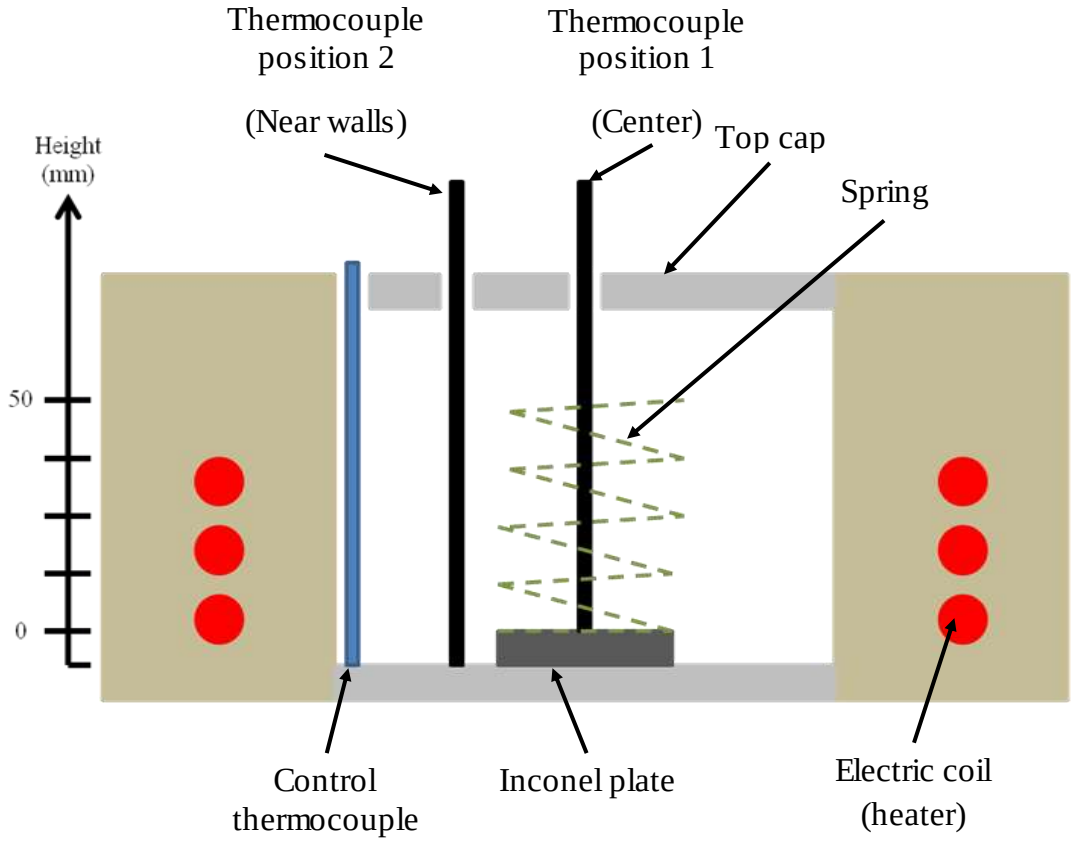

Figure 5.1. Schematic of the PPV machine for an experiment measuring the temperature at position 1 and at position 2

Figure 5.2 shows the temperature distributions along the height of the furnace for the two positions. It can be seen that the temperature profile at position 1 is inhomogeneous inside the furnace with a vertical gradient of 24°C and with a temperature higher than the 570°C targeted temperature. One possible reason to explain this higher temperature is the proximity to the heat sources. Moreover, the temperature gradient could be explained by the fact that the temperature is controlled by a thermocouple located at the very bottom of the furnace. At any time, the controller adjusts the temperature based on the control thermocouple. However, since it is placed at the bottom as opposed to the top of the furnace, the controller does not

know what the temperature is at the top of the furnace. The controller cannot adjust the temperature which could explain the temperature gradient.

The temperature profile at position 2 shows a temperature gradient of 14.1°C instead of 24°C for position 1. This time the average temperature is higher at the center than near the walls of the furnace probably due to the convection inside the furnace.

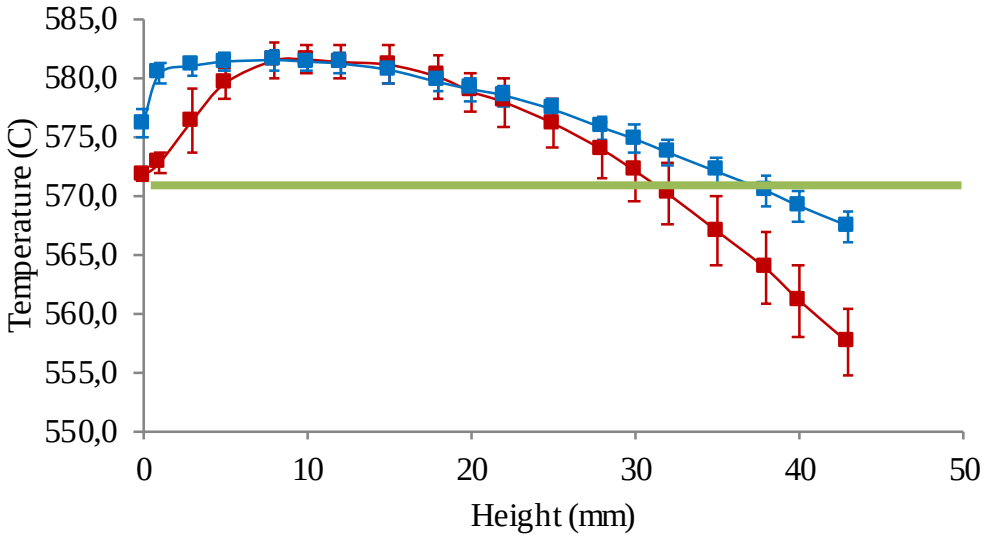

Figure 5.2. Mapping temperature near the walls of the furnace (red) and at the center (blue) at 570°C

5.2 Temperature at the center with a Pyrex® sample

The two previous experiments only give an idea of what the temperature inside the furnace is. Figure 5.3 summarizes the experiment (repeated three times) with a sample of 50mm placed at the center of the furnace.

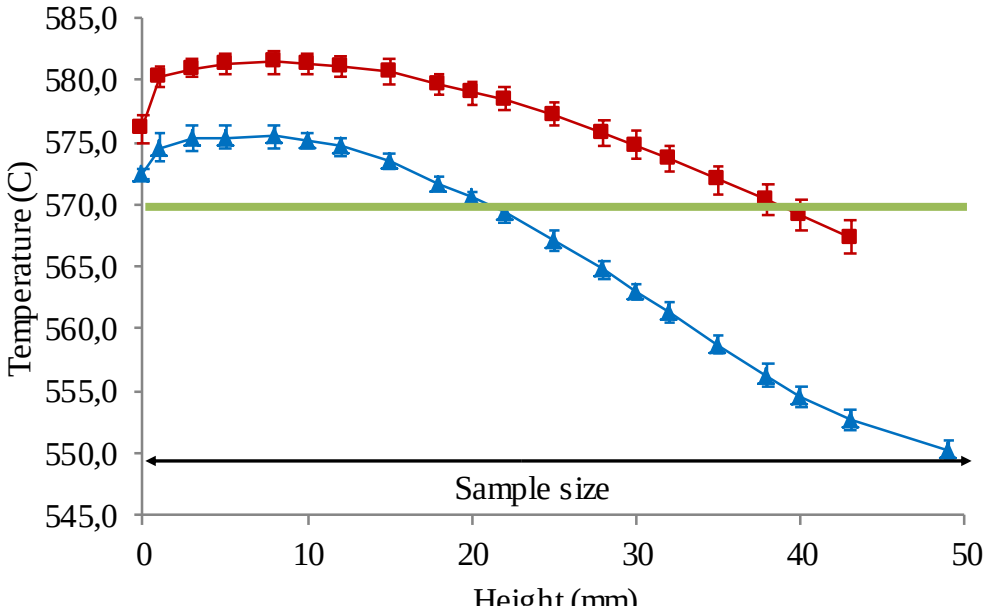

Figure 5.3. Mapping temperature at the center of the furnace with (blue curve) and without (red curve) Pyrex® spring sample at 570°C

By adding a sample in the furnace, we can observe two important results: (1) the average temperature decreases and (2) the temperature gradient increases (25.2°C) compared to the results obtained for the same experiment but without sample (temperature gradient of 14.1°C). This deviation is mainly due to the radiations emitted by the glass. Indeed, we can assume that the glass absorbs and emits thermal radiation that may tend to increase the non-uniformity of the temperature profile.

We tried to decrease the temperature gradient inside the furnace with two experiments shown in Figure 5.4. The first one consists of adding a thermal insulator (*i.e.*, glass wool) at the top and at the bottom of the furnace. The second experiment consists of adding aluminum foil inside the furnace reflecting the radiations. Figure 5.5 summarizes these results.

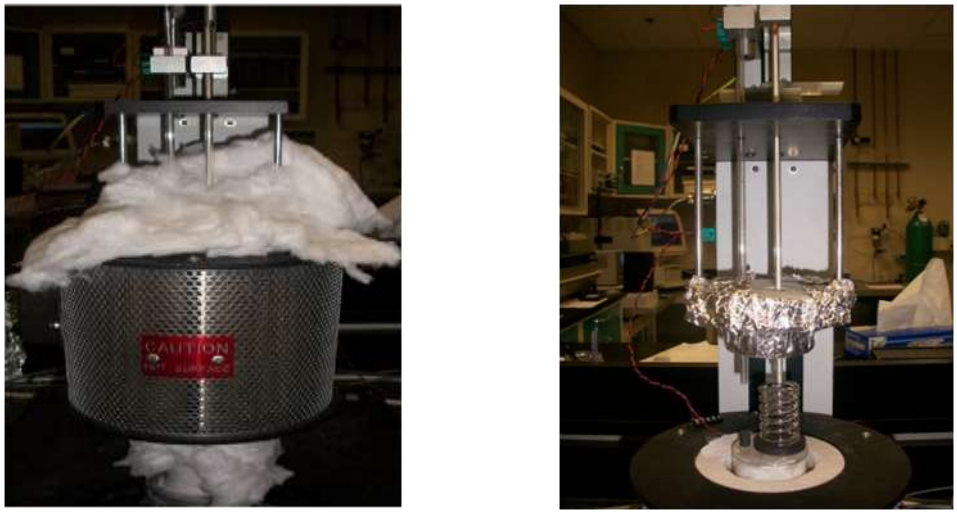

Figure 5.4. PPV machine insulates with glass wool (left) and with aluminum foil (right)

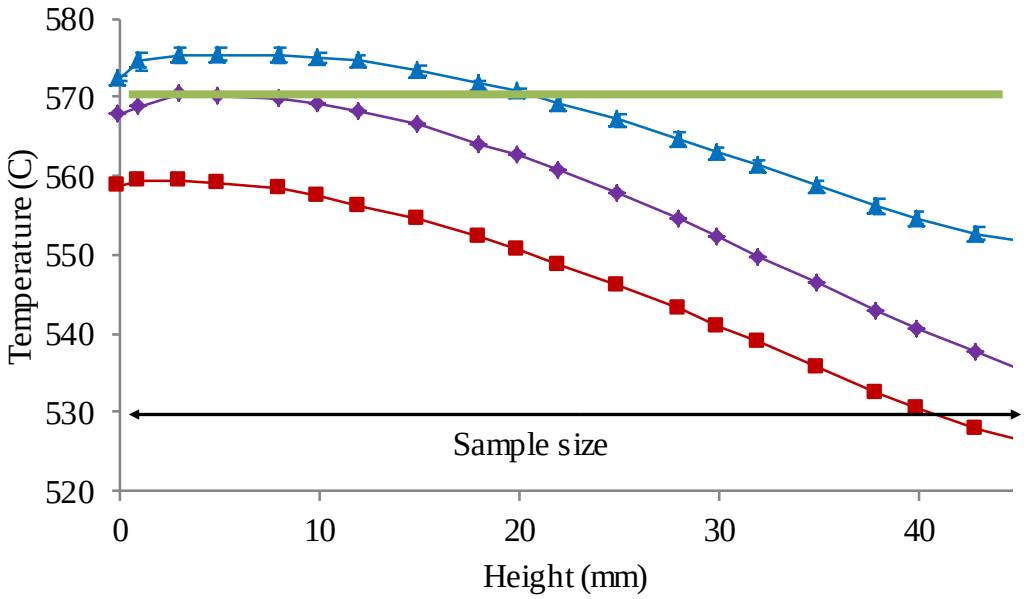

Figure 5.5. Mapping temperature at the center of the furnace with a Pyrex® sample (bleu curve), sample + insulator (red curve), sample + aluminum foil (purple curve) at 570°C

From Figure 5.5 we observe for both experiments that the temperature decreases, which was initially unexpected and we expected a temperature maybe

lower or higher than 570°C but in any case more constant. Currently, we are not able to advance a valid explanation concerning these two results other than speculating that the controller may behave differently with these two measures. Studying the thermal behavior of the furnace requires addition work such as recording the activity of the coils that are turned on and off by the controller and study the effect of convection and radiation on the glass temperature. Also, it is paramount to measure the temperature inside the glass sample as opposed to the air around the sample by drilling holes in the glass and inserting thermocouples at various locations of the sample. These tasks are part of future work.

Since we are not able to improve the temperature gradient in the furnace we decided to conduct all experiments with the furnace as designed without glass wool or aluminum foil.

CHAPTER SIX

EXPERIMENTAL RESULTS AND DISCUSSION

When the load is removed during the experiment, the spring starts to recover its original shape. In order to obtain the best response of the sample the spring must recover freely and no force must be applied on it.

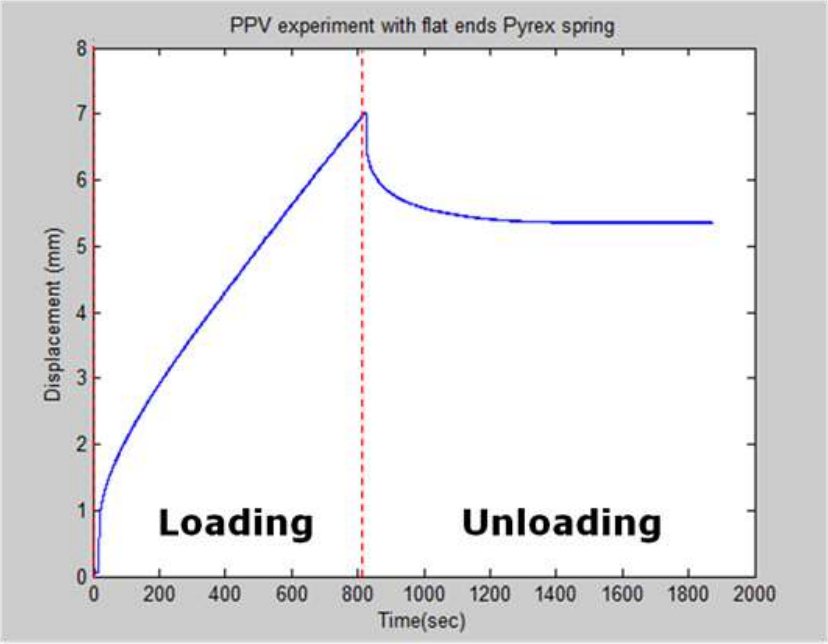

Figure 6. 1. PPV experiment with flat ends Pyrex® spring under a 500g load

6.1 External factors

Before conducting creep-recovery experiments using the PPV, the influence of several external factors on the experimental measurements due to the experimental setup and procedure has to be understood.

6.1.1 Weight offset

The LVDT, the silica rod and the top Inconel plate are directly above and rest on top of the sample. Therefore, their weight must be counterbalanced with a pulley system in order to let the spring expand freely during the recovery of the glass. A mass of 100.2 g was added to overcome this problem.

6.1.2 Friction in pulleys and steel wire

During the recovery part, the spring recovers its original shape by pushing the top plate upward. After properly counterbalancing the pulley system, the only resistive force is the pulley friction and the bending of the steel wire. This was quantified by gradually adding weight to the system until the pulley starts moving. The friction was estimated to be equivalent to a resistive force of 27mN (*i.e.*, 2.8 g), which corresponds to 0.6% of the loading force of 4.9 N (*i.e.*, 500 g).

6.1.3 Top plate rotation

When the load is applied the top plate becomes automatically in contact with the top end part of the spring. The main drawback of the spring samples is that the ends are not perfectly flat and parallel with the top and bottom plates, because of the inaccuracies of the manufacturing process. In order to account for it, each sample is tested at room temperature to measure the rotation of the top plate (see Figure 6.1). As discussed later in this chapter, the rotation of the top plate and the points of contact between the Inconel plate and the spring have shown to be a major source of uncertainty that requires additional investigation.

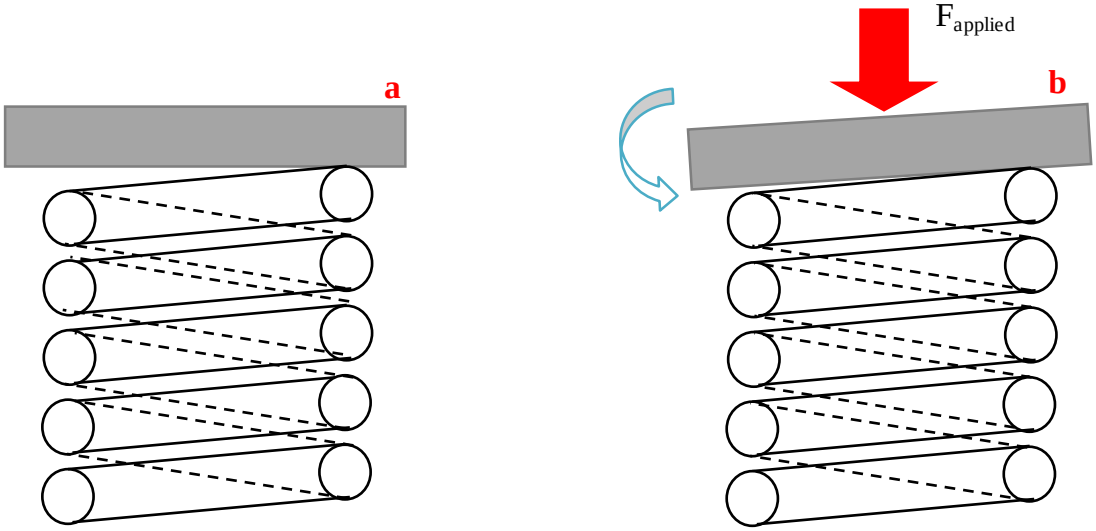

Figure 6.2. Schematic showing the position of the top plate a) with no force applied and b) with a force applied

6.1.4 Vibrations during loading and unloading

During the loading and unloading steps, the mass added has to be placed and removed from the PPV machine as quickly as possible near the LVDT at the top of the silica tube connected to the top plate. This method is not ideal since the user must be careful when adding and removing the load in order to avoid inducing vibrations in the system that would be measured by the LVDT and spoil the data.

6.2 Differential Scanning Calorimetry and X-Ray Diffraction

6.2.1 Differential Scanning Calorimetry (DSC)

We performed DSC experiments to determine a temperature range for the glass transition (T_g) of Pyrex® and to see if we observe a shift of the T_g when the glass has different thermal histories. We did three types of experiments:

1) Two DSC experiments on a virgin rod of Pyrex® before being used by the glassblower to create a spring. The rate in temperature is 25°C.min^{-1}.
2) Two DSC experiments on a piece of spring before being used in the PPV machine. The rate in temperature is 25°C.min^{-1}.
3) Two DSC experiments on a piece of spring after being used for a PPV experiment with a soaking time of two hours at 570°C. The rate in temperature is 25°C.min^{-1}.

The value of T_g is determined by taking the minimum of the time-derivative of the heat flow curve.

Figures 6.2, 6.3 and 6.4 present the results obtained during the experiments 1, 2 and 3 respectively.

Table 6.1 gives the value of T_g for each experiment.

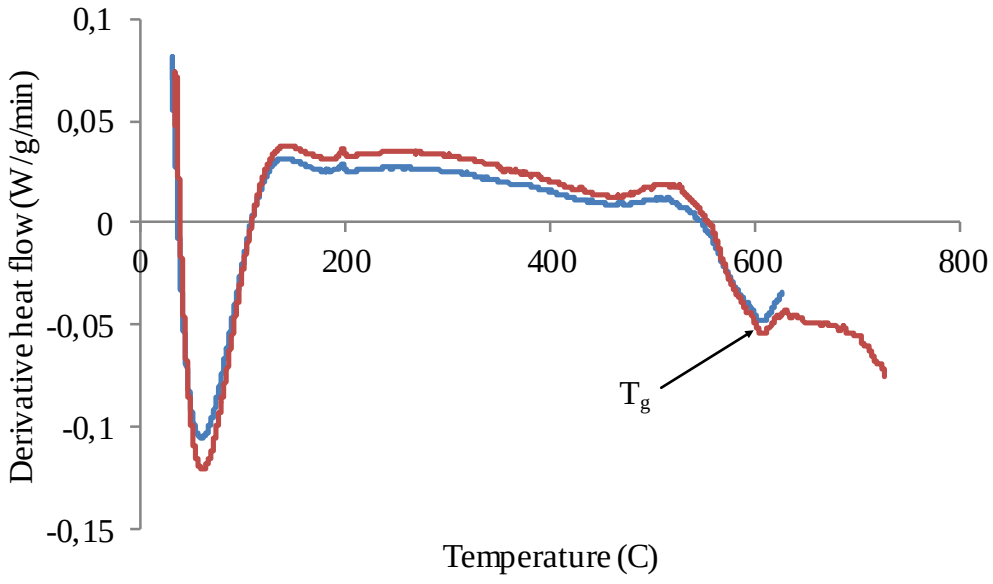

Figure 6.3. DSC results on piece of virgin Pyrex®

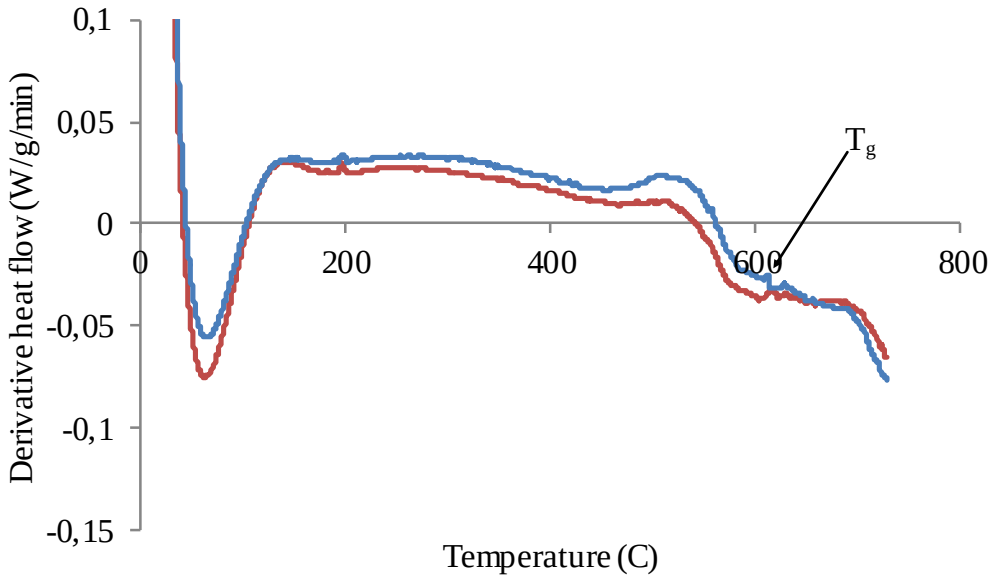

Figure 6.4. DSC results on a piece of spring before a PPV experiment

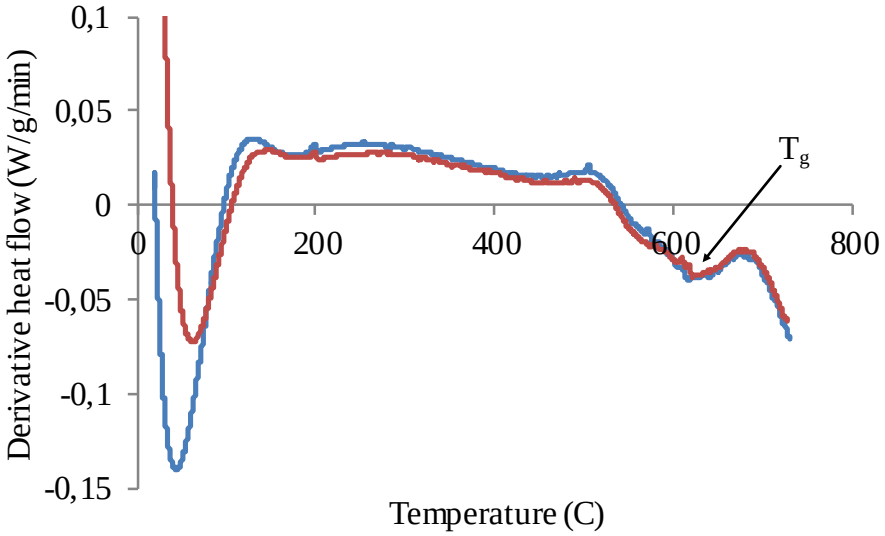

Figure 6.5. DSC results on a piece of spring after a PPV experiment with a soaking time of 2 hours at 570°C

Table 6.1. Values of T_g for the three DSC experiments

Experiment Number	1	2	3
T_g (C)	605	612	620

We can observe that after each treatment we have an increase of the T_g value. One possible explanation is the fact that Pyrex® is a phase-separated glass [15] and each thermal history on the glass will affect the value of T_g. Indeed, the two phases of Pyrex® are a SiO_2 phase and a $Na_2B_8O_{13}$ phase. The high-silica matrix phase also contains Na-borate droplets of 20-50 Angstroms. However, the presence of two phases in the glass should show two different values of T_g but only one is observed. Since the size of the droplets are small and maybe in a very low quantity we can assume that the DSC machine that we used is not accurate enough to measure the second T_g.

Figure 6.5 and 6.6 show the immiscibility dome (dash line) for the system sodium tetraborate-silica and precisely for Pyrex®. We can explain the increase of the value of T_g by the fact that we have more silica in the matrix. Indeed, for experiment 1 we measured a T_g of 605°C and the percentage of silica in the Pyrex® is approximately 80% (see Figure 6.6, point 1). When the glassblower creates the spring, the temperature of the torch is above the temperature of miscibility gap and the glass is cooled slowly after forming: we obtain a new composition for the silica-matrix and higher than 80% (see Figure 6.6, point 2). It could be explained the increase of T_g value. Then, we do a PPV experiment at 570°C for two hours. The percentage of silica in the matrix increases and consequently the value of T_g increases also (see Figure 6.6, point 3).

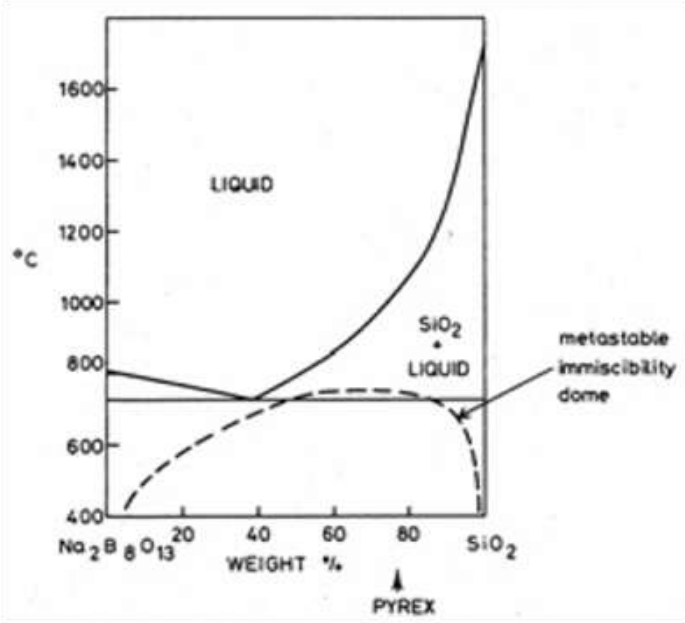

Figure 6.6. Metastable immiscibility dome in the system sodium tetraborate-silica [15]

As discussed in future work addition tests will be carried out to evaluate if this phase separation aspect of Pyrex® adversity impacts our study.

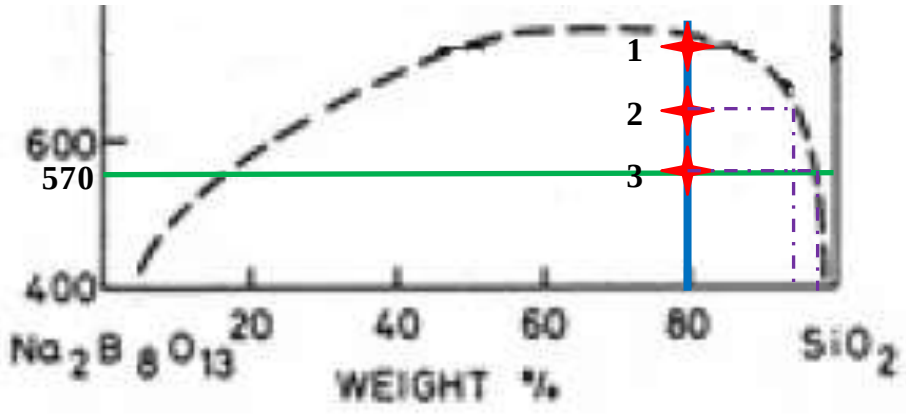

Figure 6.7. Schematic showing a possible explanation for the different value of T_g after different heat treatments

However, during the DSC experiments we use a rate of temperature of 25°C.min^{-1}. This rate has been chosen in order to increase the signal and to identify

easily the T_g value. But, if we did the same experiments with a lower rate we would observe a shift of the T_g at the lower temperature as shown in Figure 6.7. That's why, it is more correct to talk about a range of T_g than a value of T_g.

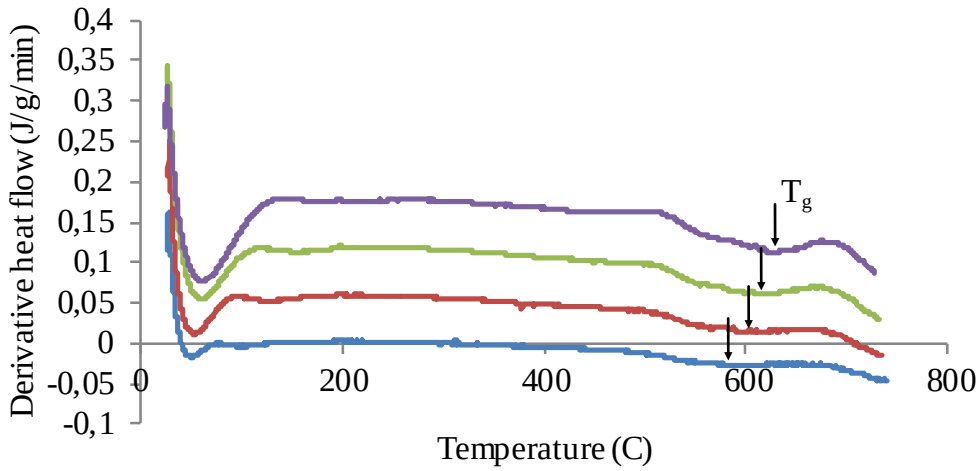

Figure 6.8. DSC experiments with different rate of temperature: 10 (blue), 15 (red), 20 (green) and 25°C.min^{-1}(purple)

6.2.2 X-Ray Diffraction (XRD)

These experiments were performed in order to know if there is some crystallization in the glass during the creep-recovery experiment. Erick Koontz – PhD student at Clemson University – performed two experiments:

1) XRD experiment on a virgin piece of Pyrex®
2) XRD experiment on a virgin piece of Pyrex® treated at 1000°C during 40 minutes.

As shown in Figure 6.8 there is no sharp peak that would denote the presence of crystallization in the glass before and after heat treatment. Therefore, there seems to be no risk to crystallize the glass during a creep-recovery experiment with the PPV.

Additional XRD experiments should be performed on samples that have been treated at higher temperatures (*i.e.*, up to 1300°C) to study the effect of the high temperature propane torch used by the glassblower to manufacture spring samples.

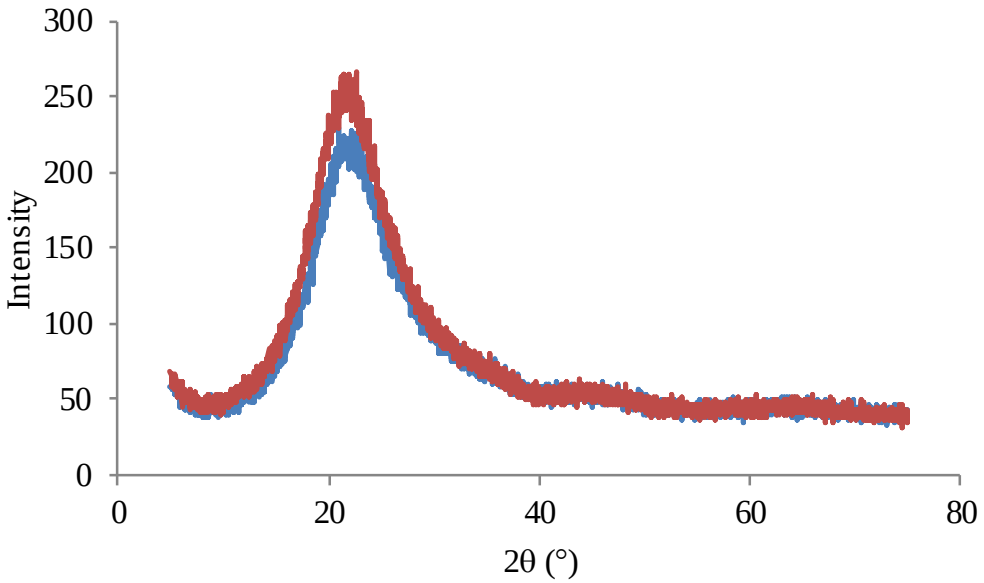

Figure 6.9. XRD results for a virgin rod of Pyrex® (blue curve) and a virgin rod of Pyrex® after a heat treatment at 1000°C during 40 minutes (red curve)

6.3 Creep-recovery experiment with a Pyrex® spring of 50mm height

6.3.1 Step-by-step procedure

Each PPV experiment follows a procedure developed empirically from the initial experiments.

1) Creep experiment at room temperature

This first experiment consists of quantifying the top plate rotation when the load is applied. The deformation measured is the sum of the elastic response of the spring and the rotation of the plate. According to Equation (2.24) we can easily

calculate the elastic response of the spring and then determine the rotation of the top plate.

Equation (2.24) is inversely proportional to the shear modulus G of the glass where G is also dependent on temperature.

2) Creep-recovery experiment

In the first step the temperature increases with a rate of $5^{\circ}C.min^{-1}$ until the target temperature ($570^{\circ}C$) is reached. During the second step, the sample is soaked inside the furnace for 2 hours, in order to have homogeneity in temperature inside and at the surface of the glass and to let the controller stabilizes the temperature (as illustrated in Figure 6.9). The third step is the loading part where a known mass (*e.g.*, 500 g or 400 g) is added to compress the spring during 15min. Finally, the load is removed in the beginning of the fourth step where the spring sample recovers partially its original shape until a steady-state is reached.

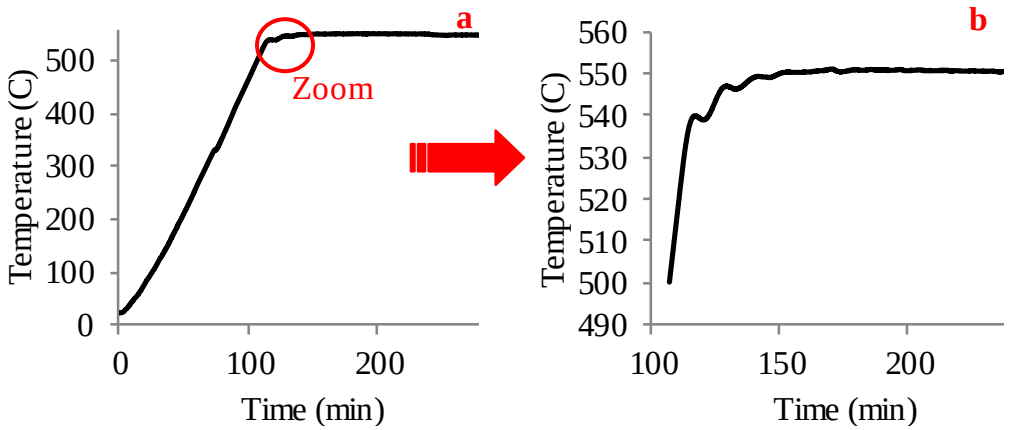

Figure 6.10. a) Ramp temperature and soaking time and b) Zoom on the stabilization region

3) Data processing

Once the creep-recovery curve is obtained from which the recovery part is extracted. The recovery part is then converted onto a retardation curve, fitted with a Prony series from which the retardation parameters are extracted. These retardation parameters will be also converted into relaxation parameters. More details are given later in this chapter.

4) Numerical analysis

After extracting the relaxation parameters, we need to correlate the results with a numerical analysis using ABAQUS, *i.e.* Finite Element Analysis (FEA) software. The properties of the material, *e.g.* Young's modulus, Poisson's ratio, temperature, and relaxation parameters are defined as input and the software calculates the elastic response of the spring, the deformation of the spring during the compression and the recovery.

6.3.2 Results

(a) Experiments repeatability

Three experiments were performed with a mass of 500g to check if we can observe repeatability between experiments. We used three springs of 50mm height in length at 570°C under a 15 min compression. The creep-recovery curves are shown in Figure 6.10.

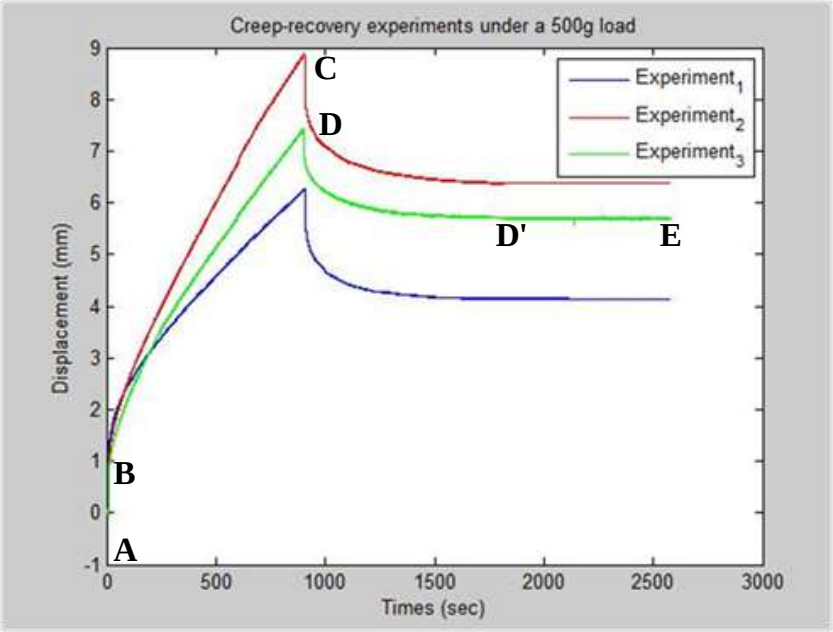

Figure 6.11. Creep-recovery experiment with a 50mm Pyrex® spring under a load of 500g at 570°C

Discussion

We can observe 3 different parts also shown in Figure 2.10 (creep-recovery experiment under tensile stress):

- Segments [AB] & [CD] which correspond to the elastic response of the spring and the top plate rotation.
- Segment [BC] which is the time-dependant loading response, *i.e.* the spring is compressed.
- Segment [DE] which represents the strain delayed part, *i.e.* the recovery of the glass when no force is applied. We can also observe that segment [D'E] is constant. This shows that we have reached the steady-state and the glass does not recover anymore.

However, we can see there is no repeatability among these three experiments even though the three spring samples had the same geometry (50mm height and 4 active coils) and the load (m=500g), and the temperature (570°C) were also the same, we obtain three different creep-recovery curves. We compared the loading parts and recovery parts (tabulated in Table 6.2) and we observed that while the loading parts are significantly different, the recovery values are fairly close.

Table 6.2. Recovery values for 3 experiments under a 500g load

	Experiment 1	**Experiment 2**	**Experiment 3**
Elastic response + top plate rotation + compression (mm)	6.274	8.880	7.418
Recovery (mm)	1.4251	1.4272	1.2610

We tried to understand why we did not obtain the same compression value of each experiment and our first explanation is the load is not applied at the center of the spring due to the irregular shape of the top coil of the spring. The point of contact between the top plate and the coil is likely to be off-center, which creates a bending moment in the spring in addition to the vertical compressive force. The variations in the location of the points of contact among samples may is therefore expected to create the non-repeatability of the results shown in Figure 6.10. To validate this explanation we used the FEA sofware ABAQUS to model the spring. We did five different simulations by changing the location of the load as shown in Figure 6.11. The coordinates of each location are given below in terms of the radius of the spring (r) and the pitch of the coil (p).

- Position 1: Center of the spring (0,0,0)

- Position 2: Half radius of the spring (-r/2,0,0)
- Position 3: Radius of the spring (-r,0,0)
- Position 4: Radius of the spring (r,0,p/2)
- Position 5: Radius of the spring (0,-r,3p/4)

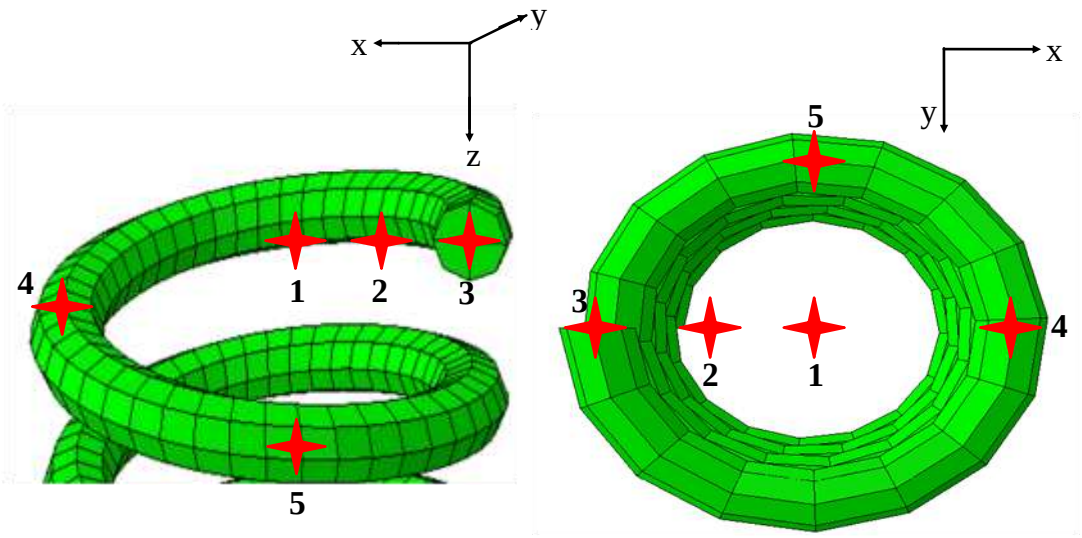

Figure 6.12. Position of the load on the spring for the five simulations in ABAQUS

(b) Numerical analysis

Figure 6.12 shows the spring drawn with Solidworks (3D CAD design software) and used with ABAQUS. The coloring shows the stress level within the spring.

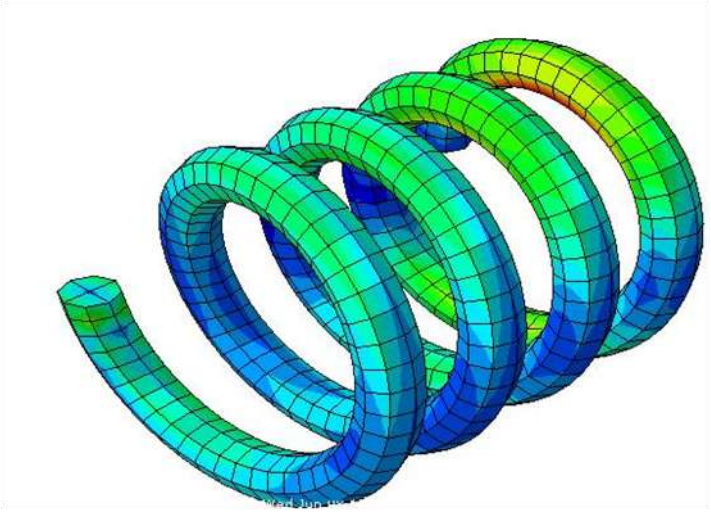

Figure 6.13. Spring with four active coils in ABAQUS

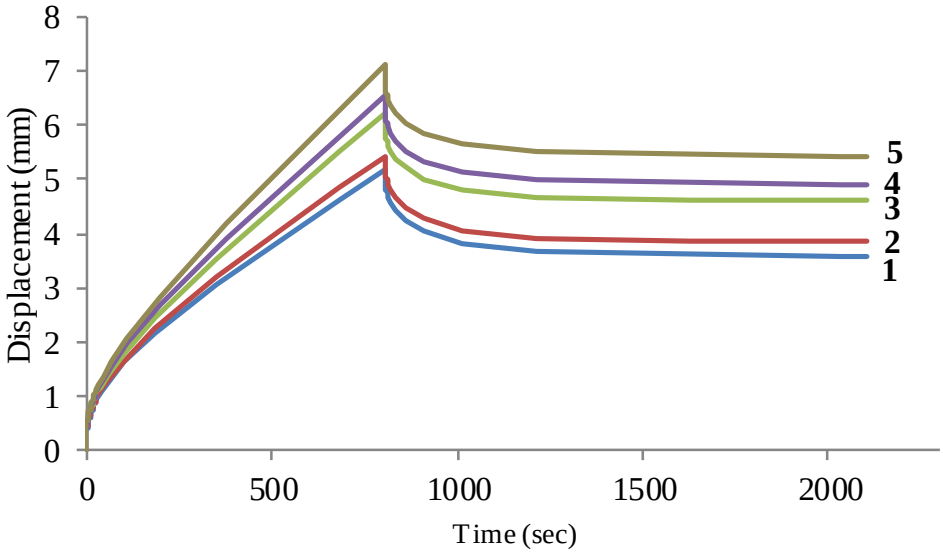

Figure 6.14. Numerical analysis with ABAQUS for a load at position 1 (blue curve), position 2 (red curve), position 3 (green curve), position 4 (purple curve) and position 5 (brown curve) under a 500g load at 570˚C.

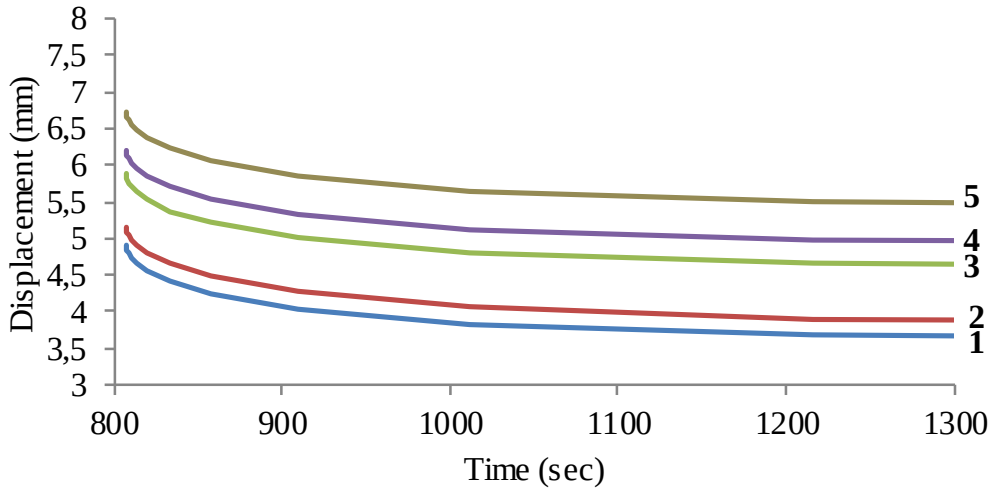

Figure 6.15. Numerical analysis with ABAQUS showing the recovery for a load at position 1 (blue curve), position 2 (red curve), position 3 (green curve), position 4 (purple curve) and position 5 (brown curve) under a 500g load at 570°C.

It can be seen that by changing the position of the load from the center to the edge of the spring, the deformation of the loading part increases (by up to 40%) while the recovery part is fairly constant (within 3%). This may validate the explanation for the non-repeatability of the loading part under the same load (500g). Table 6.3 summarizes the results obtain with the numerical analysis.

Table 6.3. Numerical analysis results on ABAQUS for different load positions at 570°C

Load position	Position 1 (blue curve)	Position 2 (red curve)	Position 3 (green curve)	Position 4 (purple curve)	Position 5 (brown curve)
Elastic response + Compression (mm)	5.182	5.432	6.215	6.571	7.123
Recovery (mm)	1.326	1.312	1.283	1.298	1.296

Since the extraction of the retardation parameters is exclusively based on the recovery part, the non-repeatability of the loading part is acceptable.

(c) Retardation curve

Once the creep-recovery curve is obtained experimentally, it is converted into a retardation curve by following four steps:

1) Extract the recovery part from the creep-recovery curve (elastic response + top plate rotation + recovery)

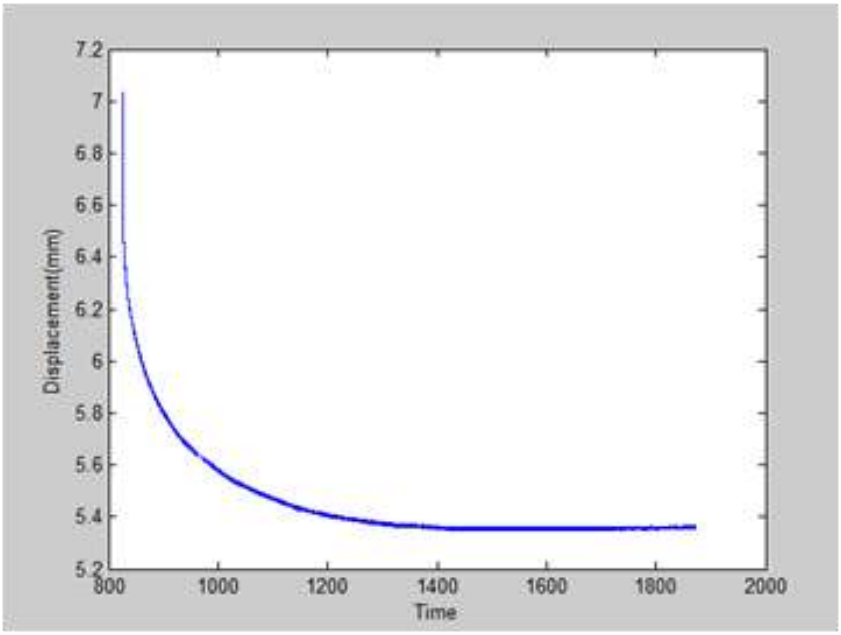

Figure 6.16. Elastic response + top plate rotation + recovery

2) Remove the value of the elastic response and the top plate rotation in order to obtain only the recovery of the glass.

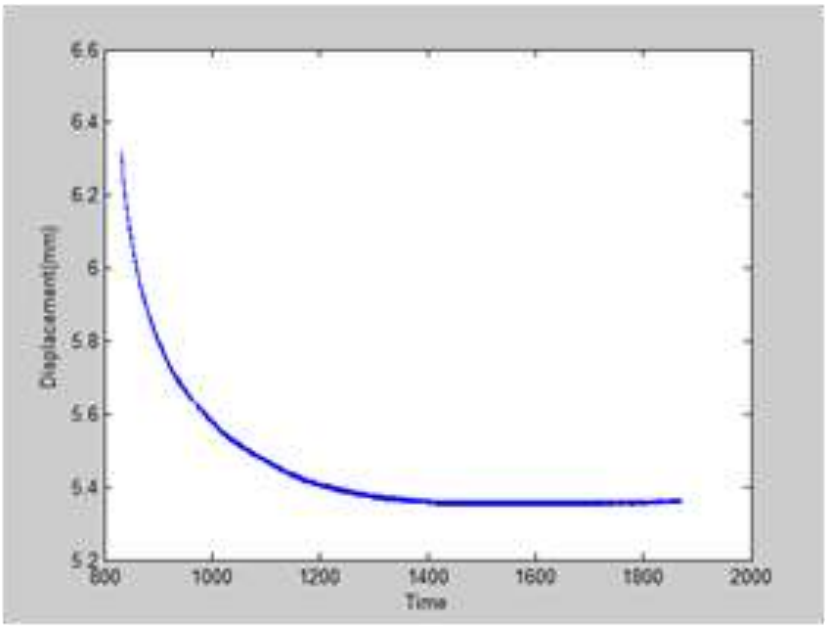

Figure 6.17. Recovery curve

3) Normalize the displacement in order to obtain the normalized recovery curve. The normalization is achieved by scaling the curve with the difference between the maximum and the minimum values of the recovery curve. The normalized recovery curve is then between 0 and 1.

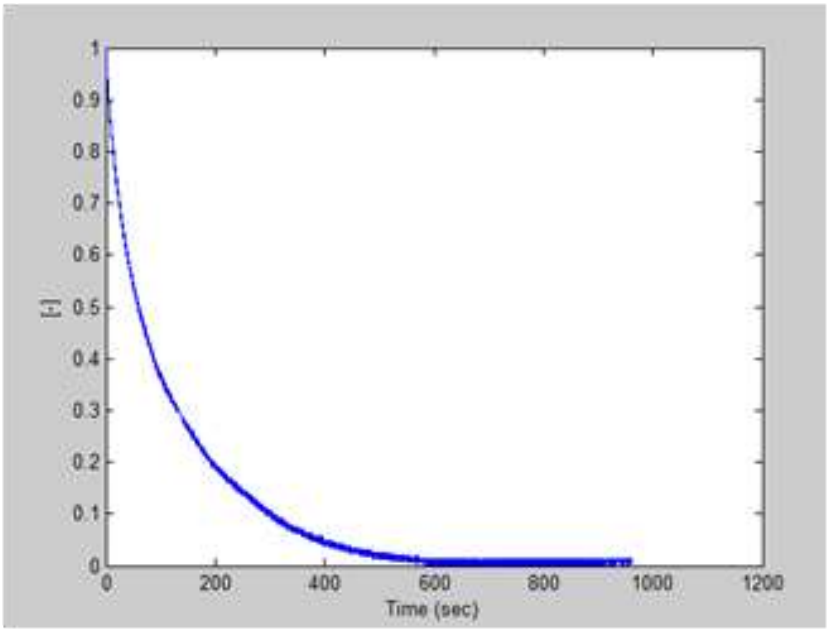

Figure 6.18. Normalized recovery curve

4) Convert the time scale into logarithmic time scale to obtain the retardation curve. This curve will be fit with the Prony Series.

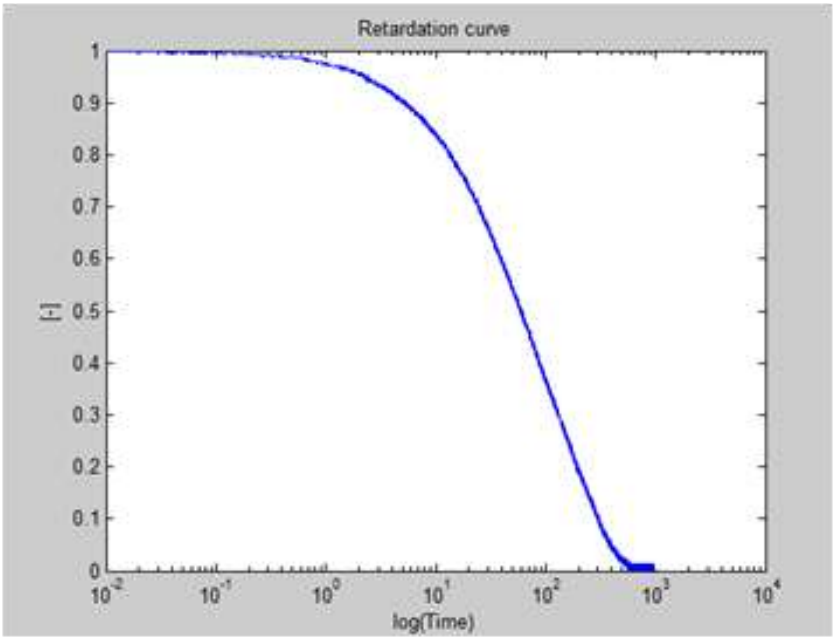

Figure 6.19. Retardation curve in semi log scale

The four steps were applied to the three experimental data obtained for 500g load. Figure 6.18 shows that the retardation curves are slightly different. The main explanation for this deviation could be due to the fact that the load is never applied in the same location on the spring which may affect the elastic response and the top plate rotation. This inaccuracy can change the curvature of the retardation curve.

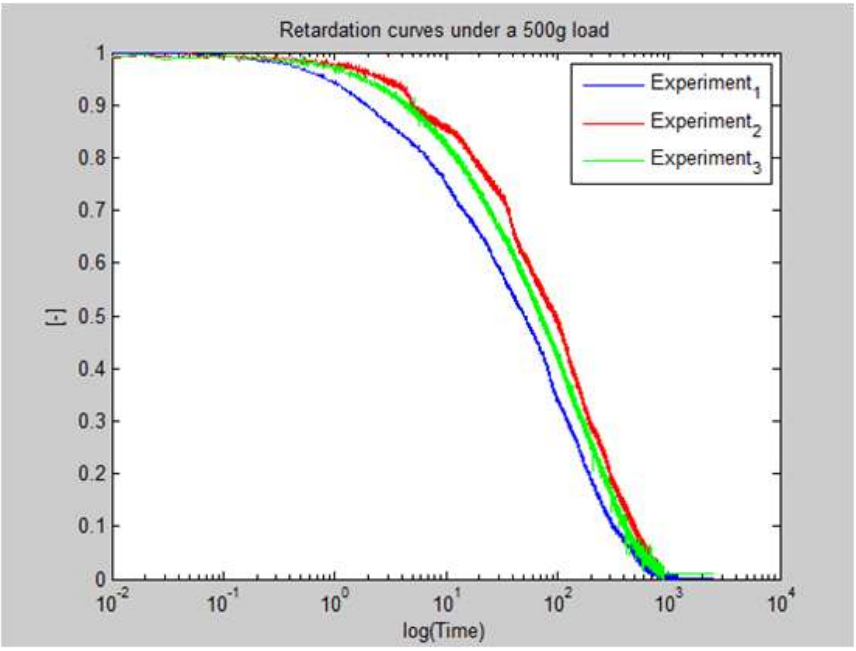

Figure 6.20. Retardation curves for the three experiments under a 500g load

Since we did not obtain exactly the same retardation curves we decided to use an average retardation curve which is then fitted with the Prony series.

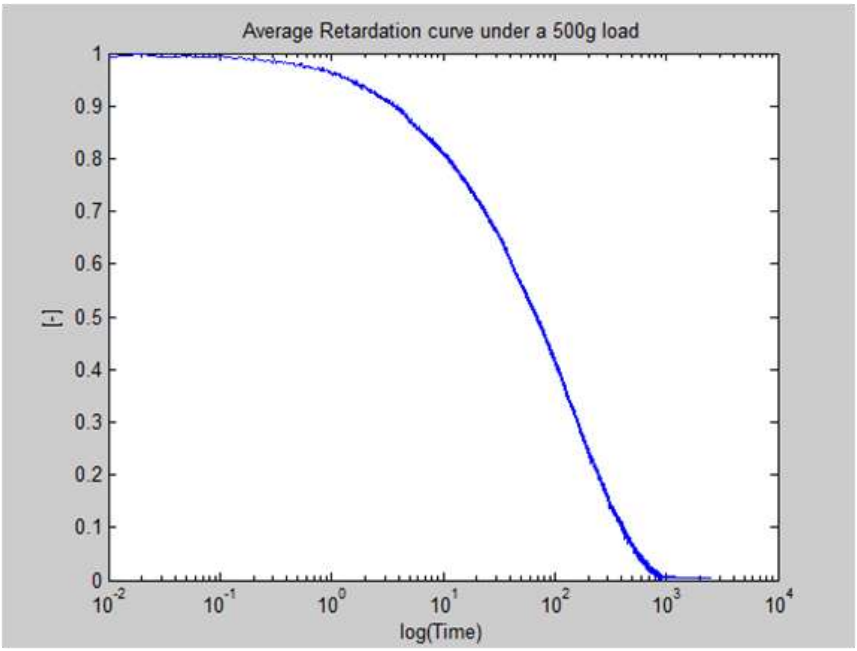

Figure 6.21. Average retardation curve under a 500g load

6.4 Extraction of pure shear retardation parameters

Once we obtain the retardation curve, we need to fit it with a Prony Series which describes the generalized Maxwell model. A Matlab program was created for this major part by a former student at Clemson University [5]. The input data of the program are some arbitrary retardation times λ_{1j} (j=1…N) where N_1 is an arbitrary number of terms. The output of the program includes the retardation weights ν_{1j}. Inside the program, an optimization function has been programmed which tries to find the best retardation weight ν_{1j} corresponding to the retardation time λ_{1j} in order to minimize the deviation with the experimental data. Equation 6.1 describes mathematically the optimization function:

$$Minimize \sum_{k=1}^{n}(\phi(t_k) - \sum_{j=1}^{N} \nu_{1j}\exp(-\frac{t_k}{\lambda_{1j}}))^2 \qquad (6.1)$$

where n is number of experimental data points (*e.g.*, n=10 000), N number of terms in the Prony Series (*e.g.*, N=5), and $\phi(t_k)$ is the experimental retardation function.

To run the program we need in input data the retardation time λ_{1j}. A first set of data chosen arbitrarily has been tested and only the retardation times with a retardation weight ν_{1j} bigger than 1.10^{-6} were kept. The Matlab program is run a second time until the experimental data are correctly fitted by the Prony Series. Table 6.4 shows the retardation parameters fitting the average retardation curve (Figure 6.22) for a load of 500g.

Table 6.4. Retardation parameters fitting a retardation curve for a 500g load

Retardation time λ_{1j}	Retardation weight ν_{1j}
1	0.041789
10	0.058519
19.63	0.161703
144.37	0.5618225
380	0.1754636

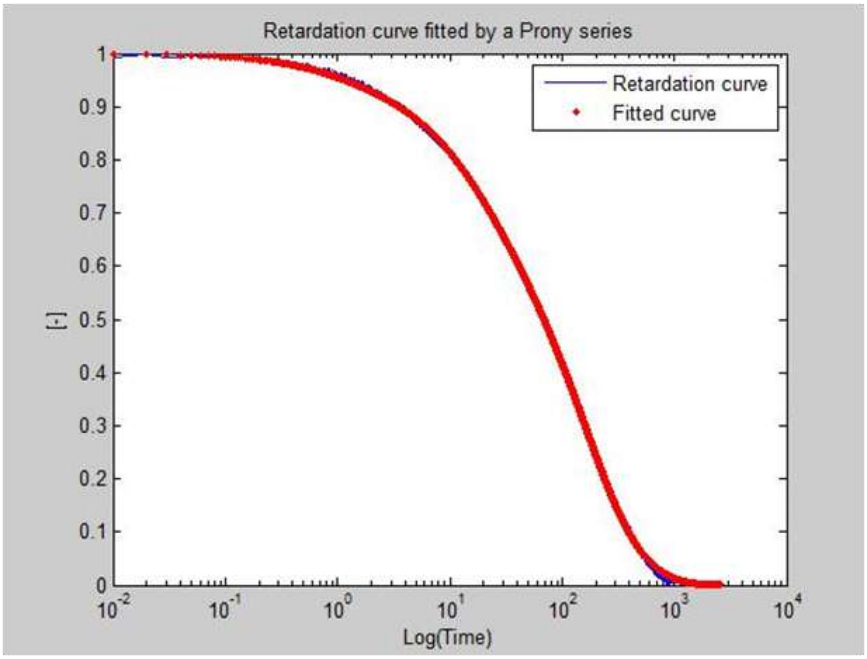

Figure 6.22. Retardation curve fitted by a Prony series for Pyrex® at 570°C

6.4.1 Conversion of retardation parameters into relaxation parameters

Gy *et al.* [16] developed a mathematical procedure necessary to convert the retardation parameters into relaxation parameters. Some viscoelastic constants are needed [17] [18] to determine the relaxation parameters. A Matlab program was created to solve the following equations.

1) The relaxation viscoelastic moment $< \tau_1 >$ is defined by a relationship between the viscosity η and the shear modulus G:

$$< \tau_1 >= \frac{\eta}{G} \tag{6.2}$$

In our case, the difficulty presented by the equation above is the fact that we need to know the viscosity of the glass. The viscosity is strongly dependent of the temperature and we have a temperature gradient in the furnace. However, we do not know what the temperature is inside the sample (see future work). According to Figure 6.7 we know that the temperature of transition region of Pyrex® is around 570°C. The assumption that we did for the calculation of the relaxation parameter is the following:

We considered that the lower 22mm of the spring are expected to have a temperature equal to or above than 570°C (see Figure 5.3) and consequently the viscosity is lower than the higher part of the spring. The lower 22mm could be consider more "liquid" and the higher part more "solid" and during the creep-recovery test the lower part will compress more than the second one.

The average temperature for the lower 22mm is 573.5°C and according to Figure 6.23 the viscosity is $10^{12.28}$ Pa.s. In this thesis we assume that the temperature of the glass is the same as that of the air. However, this may induce inaccuracy that will be resolved as part of future work.

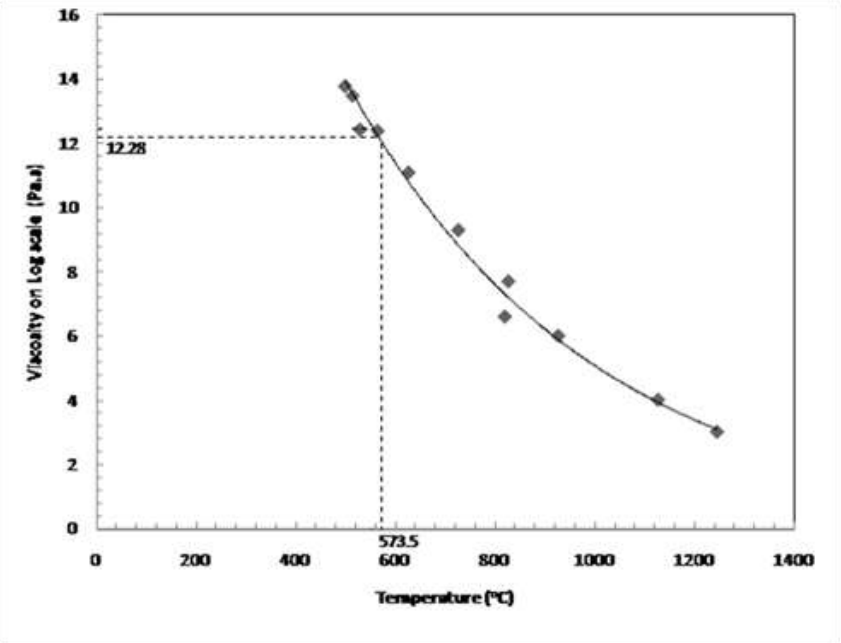

Figure 6.23. Viscosity curve for Pyrex® [18] [19]

2) The relaxation viscoelastic constant is defined as the total delayed strain, *i.e.* recovery and the instantaneous elastic response of the spring.

$$\frac{<\tau_1^2>}{<\tau_1>^2} = \frac{\delta_{recovery} - \delta_{instantaneous}}{\delta_{instantaneous}} \tag{6.3}$$

To obtain the (m+1) relaxation times we need to solve a polynomial equation of order (m+1), in term of the variable p, where m is the number of retardation parameters. The negative reciprocals of the (m+1) values of p give the relaxation times τ_{1j}.

$$-p^2\phi_1(p)\left(\frac{<\tau_1^2>}{<\tau_1>^2} - 1\right) + p\left(\frac{<\tau_1^2>}{<\tau_1>^2}\right) + \left(\frac{1}{<\tau_1>}\right) = 0 \tag{6.4}$$

where $\phi_1(p)$ is defined by:

$$\phi_1(p) = \sum_{j=1}^{m} \frac{\lambda_{1j}}{1 + \lambda_{1j}p} \nu_{1j} \tag{6.5}$$

Once the relaxation times are found, they are used to determine the relaxation weights ω_{1j} by solving a system of (m+1) equations.

$$\Psi_1\left(-\frac{1}{\lambda_{1k}}\right)=\sum_{j=1}^{m}\frac{\tau_{1j}}{1-\frac{\tau_{1j}}{\lambda_{1k}}}\omega_{1j}=0 \tag{6.6}$$

k=1…m

$$\Psi_1(0)=\sum_{j=1}^{m}\tau_{1j}*\omega_{1j}=<\tau_1> \tag{6.7}$$

Table 6.5 shows the relaxation parameters after applying the method describes by Gy *et al*.

Table 6.5. Relaxation parameters of Pyrex® at 573.5°C

Relaxation times τ_{1j}	Relaxation weight ω_{1j}
0.801375	0.214625
6.512016	0.380140
13.518012	0.098150
57.346681	0.198280
307.726579	0.032939
641.308711	0.075867

6.4.2 Relaxation parameters for a creep-recovery experiment under 400g load

We did exactly the same experiments described above for a load of 500g but this time with a load of 400g. The goal of these experiments was to compare the relaxation parameters and checked the expect linearity of the glass [6], *i.e*. the stress

increases in proportion to the strain; we expect to measure the same retardation curve under a load of 400g as for a under a load of 500g.

We observed the same problem as mentioned in the experiment with a 500g load: different compressions maybe due to the position of the load during the test. An average retardation curve has been created, and then fitted with a Prony series. Retardation and relaxation parameters are shown in Table 6.6.

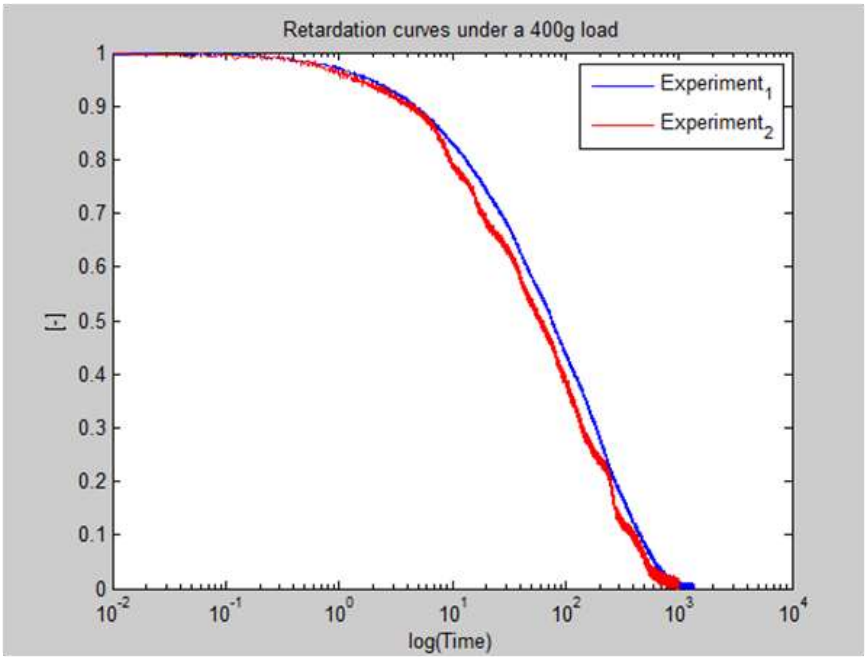

Figure 6.24. Retardation curves for the two experiments under a 400g load

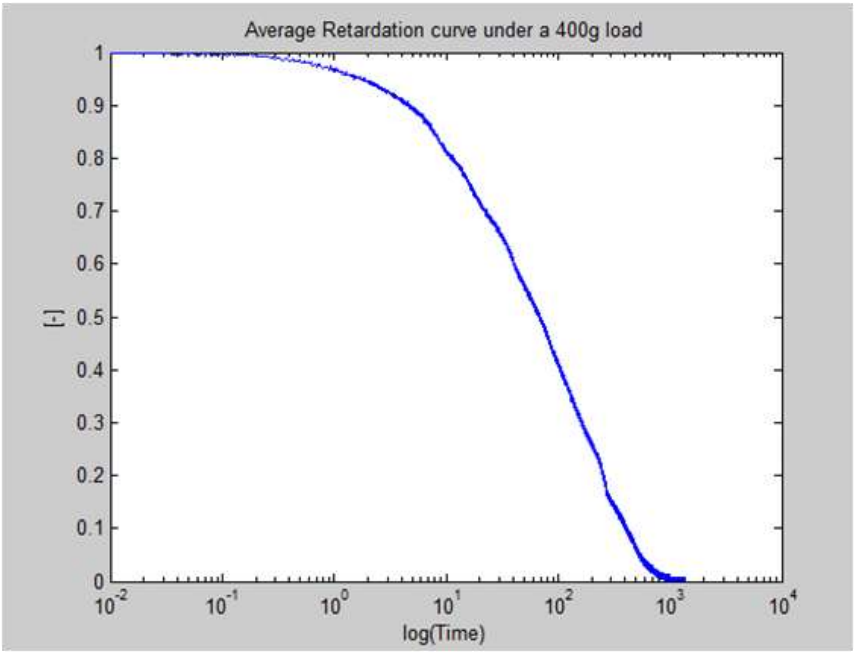

Figure 6.25. Average retardation curve under a 400g load

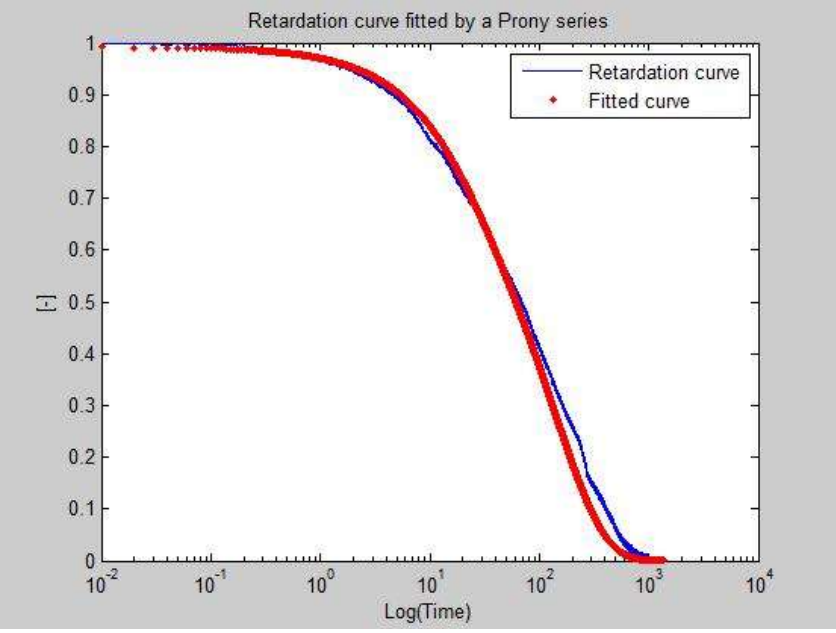

Figure 6.26. Average retardation curve under a 400g load fitted with a Prony series

Table 6.6. Retardation and relaxation parameters at 573.5°C

Retardation times λ_{1j}	Relaxation weight ν_{1j}	Relaxation times τ_{1j}	Relaxation weight ω_{1j}
		0.937520	0.072530
1	0.0070274	5.534432	0.718003
10	1e-006	10.000053	0.000003
19.63	0.23982	52.961929	0.125686
144.37	0.7393074	377.910025	0.000683
380	0.005472593	821.417820	0.083095

Compared to the results obtain with 500g, we can see that we do not obtain exactly the same results. Several explanations could explain this difference:

1) The fit for the 400 g retardation curve is not as good for the 500g retardation curve and therefore we do not have the same retardation parameters.
2) We have some differences in the retardation curves due to the experiment and the inaccuracy with the load position.

6.4.3 Comparison of the stress relaxation results obtain with a creep-recovery experiments under tensile stress

The former student at Clemson University studied stress relaxation of Pyrex® glass under tensile stress. The goal of this section is to compare the results obtained between the two methods (tensile and compressive stresses) and to formulate an explanation on the differences observed. Figure 6.26 summarizes the results.

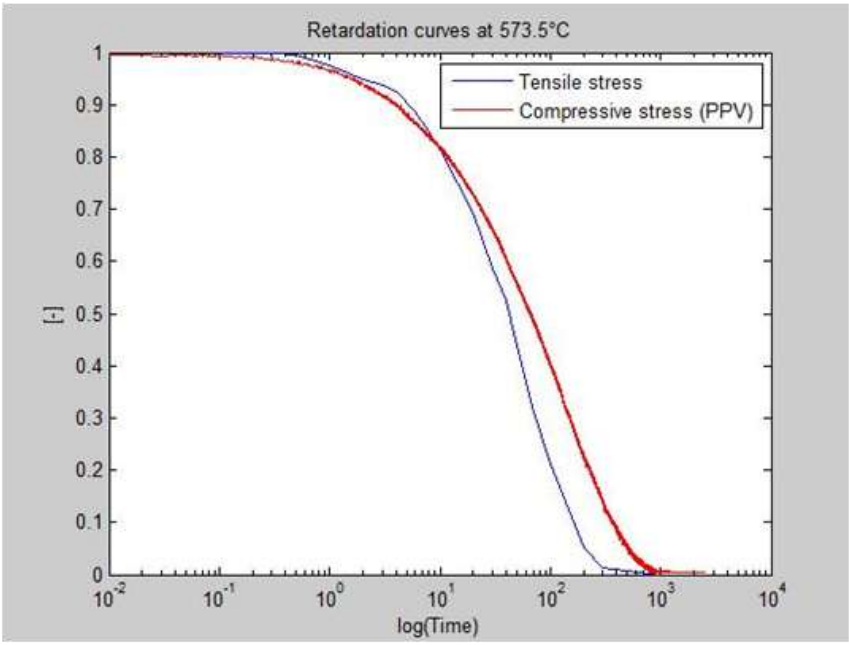

Figure 6. 27. Retardation curves obtained after a creep-recovery experiment under tensile stress (blue curve) and compressive stress (red curve)

As shown on Figure 6.27 we can see that we do not obtain the same results. There can be several explanations:

1) For the creep-recovery experiment under compressive stress there is a temperature gradient of 25°C inside the furnace which is not the case for the experiment under tensile stress (*i.e.*, the temperature gradient is only 3°C). There is inaccuracy in the temperature for the first case and will affect the viscosity and then the stress relaxation parameters.
2) For both cases, a rotation from the top plate for the PPV or from the spring in the case of the experiment under tensile stress is measured. If the rotation is not well known, there is an uncertainty on the value of the instantaneous response and then on the curvature of the retardation curve.

CHAPTER SEVEN

CONCLUSION AND FUTURE WORK

7.1 Conclusion

The intent of this thesis was to present a new method for the determination of pure shear retardation parameters using a Parallel Plate Viscometer (PPV) machine. This research is part in a larger project focused on studying precision glass molding (PGM) where the grasp of stress relaxation is an important parameter to control the accurate lens shape.

The advantage of using the PPV machine is its simplicity in conducting creep-recovery experiments. The major part of the problems encountered during this research has been understood. Nevertheless, some difficulties have to be resolved to improve accuracy in the measurement, such as the temperature gradient inside the furnace and the uncertainty in the load position during the loading part. Despite these issues, the method for calculating the stress relaxation parameters was implemented. Complementary to the experimental measurements a simulation using Finite Element Analysis (FEA) software was created to verify the results obtained experimentally.

7.2 Future work

After a year working on the PPV machine, we are able to determine a list of tasks to continue the work started.

1) Even though the temperature gradient in the air in the furnace is well known, the temperature inside the glass needs to be properly characterizes in order to increase confidence in determination of the viscosity. This could be done by inserting thermocouples inside the glass sample at different locations.
2) We need to obtain a better control of the load position since it changes significantly during the compression and ultimately affects the interpretation of the recovery data.
3) Once the pure shear stress relaxation parameters are determined, a new set of experiments must be performed to determine the hydrostatic stress relaxation parameters. This is usually done using a uniaxial test, which includes both shear and hydrostatic behaviors.
4) Since the project is focused on the precision glass molding process of specific types of glass, the stress relaxation characterization method must be applied to the optical glasses of interest such as N-BK7® and L-BAL35®. These glasses are known as low-T_g glasses and are generally more difficult to work with than Pyrex®.

REFERENCES

[1] P. Mossadegh, "Friction measurement in precision glass molding", PhD, Clemson University, South Carolina, 2010.

[2] S. Rekhson, "Viscosity and stress relaxation in commercial glasses in the glass transition region", *Journal of Non-Crystalline Solids* 38 & 39 (1980), 457-462.

[3] L. Duffrene, R. Gy, H. Burlet, R. Piques, "Multiaxial linear viscoelastic behavior of a soda-lime-silica glass based on a generalized Maxwell model", *Journal of Non-Crystalline Solids*, Vol. 215, 208-217, 1997.

[4] J.E. Shelby, "Introduction to Glass Science and Technology", the Royal Society of Chemistry, ISBN 0-85404-639-9, 2nd Ed. (2005)

[5] H. Kadali, "Experimental characterization of stress relaxation of glass", Master thesis, Clemson University, South Carolina, 2009

[6] G. W. Scherer, "Relaxation on glass and composites", John Wiley and Sons, Inc, ISBN 0-89464-643-5, 2nd Ed. (1992)

[7] R. C. Hibbeler, "Mechanical of Materials", Pearson Prentice Hall, ISBN 0-13-191345-X, 6th Ed. (2005)

[8] G. Richard, J. Bundynas, K. Nisbett, "Shigley's Mechanical Engineering Design", McGraw-Hill, ISBN 978-007-125763-3, 8th Ed. (2008).

[9] http://www.sceram.com

[10] S. Gaylord, "Thermal and structural properties of candidate moldable glass types", Master thesis, Clemson University, South Carolina, 2008

[11] http://www.glassdynamicsllc.com

[12] http://www.foctek.net

[13] http://www.uqgoptics.com

[14] http://www.ohara-gmbh.com

[15] T. J. Rockett, W. R. Foster, "The system Silica-Sodium Tetraborate", *Journal of the American Ceramic Society*, Vol. 49, 30-33, 1966

[16] R. Gy, L. Duffrene, M. Labrot, "New insights into viscoelasticity of glass", *Journal of Non-Crystalline Solids*, Vol. 175, 103-117, 1994

[17] L. Duffrene, R. Gy, "Viscoelastic constants of a soda-lime-silica glass", *Journal of Non-Crystalline Solids*, Vol. 211, 30-38, 1977

[18] S. Rekhson, "Viscosity and stress relaxation in commercial glasses in the glass transition region", *Journal of Non-Crystalline Solids 38 & 39*, 457-462, 1980

[19] M. J. Pascual, L. Pascual, A. Dran, "Determination of the viscosity-temperature curve for glasses on the basis of fixed viscosity point determined by hot stage microscopy", *Physics and Chemisty glasses*, Vol. 39, 113-118, 1955

APPENDICES

Appendix A

Temperature-dependent mechanical properties of Pyrex® glass

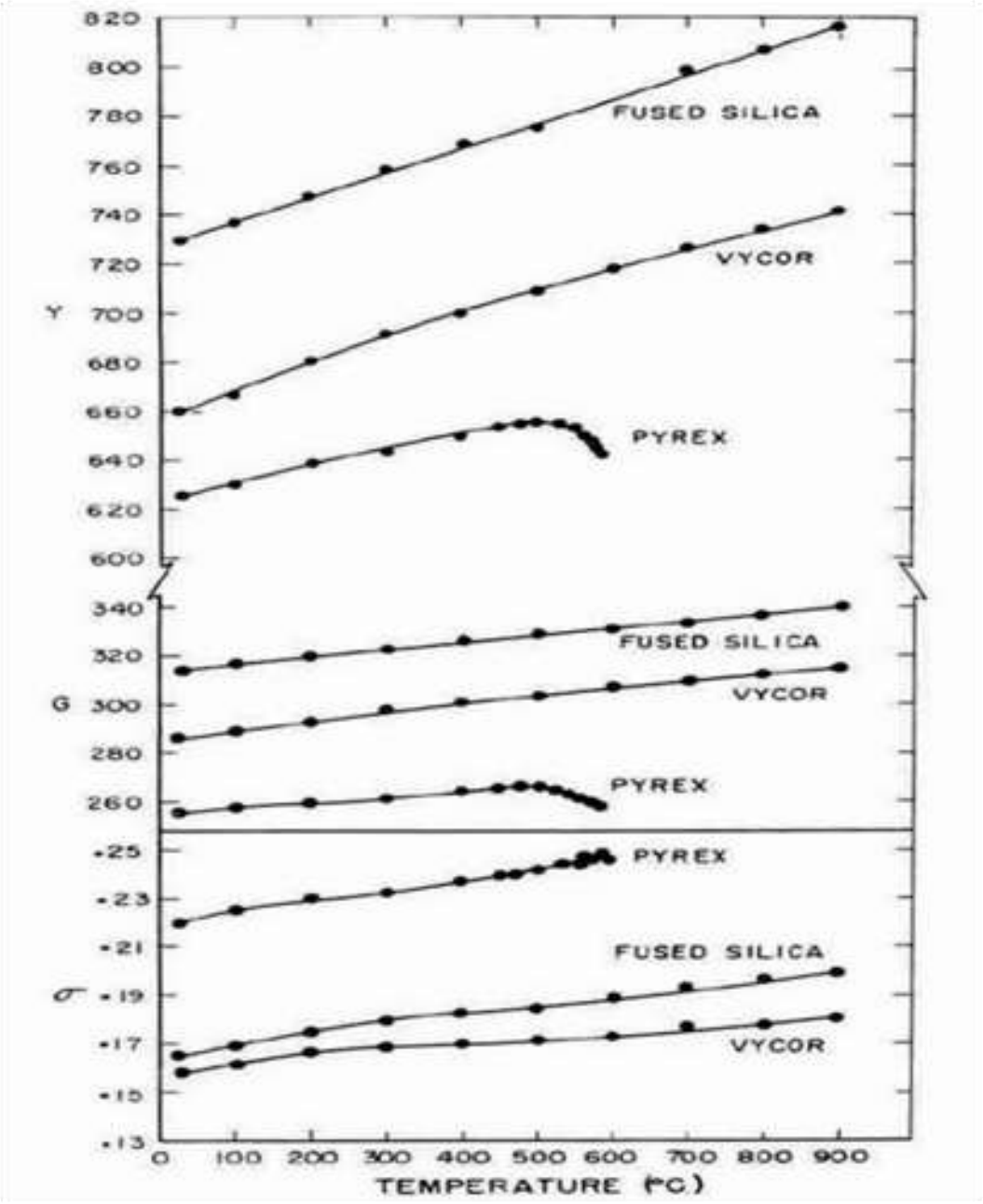

Appendix B

Matlab program for the conversion of retardation parameters into relaxation parameters

```
clear all

fprintf('\n');
Ed=input('Total delayed elasticity value Ed (mm): ');
fprintf('\n');
Ei=input('Instantaneous elastic response value Ei (mm): ');
fprintf('\n');
RVC=(Ed+Ei)/Ei;

G=input('Shear modulus value (GPa): ');
fprintf('\n');
G1=G*10^9;
n=input('Viscosity value (log(Pa.s)): ');
fprintf('\n');
n1=10^n;
fprintf('|-----------------------------------------------------------
-------------------------------------|\n')
fprintf('| Delayed strain |Instantaneous response|   (Ed+Ei)/Ei (RVC)
|   Shear modulus     |Log(Viscosity)|\n');
str = fprintf('|  %d |   %d      |   %d     |   %d     |%d |\n',
Ed,Ei,RVC,G1,n1);
fprintf('|-----------------------------------------------------------
-------------------------------------|\n')

Parameter=input('How many retardation time do you want: ');
fprintf('\n');

if Parameter==1
    rt1=input('1st retardation time: ');
    rw1=input('1st retardation weight: ');
    a=[rt1;rw1;RVC;G1;n1];
    syms x
    f=(-x*x)*((a(1)*a(2))/(1+a(1)*x))*(a(3)-
1)+(x*a(3))+((a(4))/(a(5)));
    y=solve(f,x);
    solnvalue=double(y);
    rlt1=-1/(solnvalue(1));
    rlt2=-1/(solnvalue(2));
    A=[(rlt1/(1-rlt1/rt1)) (rlt2/(1-rlt2/rt1));rlt1 rlt2];
    B=[0;n1/G1];
    S=inv(A)*B;
    Sum_rlwi=S(1)+S(2);
    Sum_rwi=rw1;
    fprintf('|-----------------------------------------------------------
---------------------------|\n')
fprintf('| Retardation time |Retardation weight|   Relaxation time  |
Relaxation weight     |\n');
```

```
str = fprintf('|        %.6f    |       %.6f      |    %.6f          |
%.6f                 |\n', rt1,rw1,rlt1,S(1));
str = fprintf('|                    |                  |     %.6f
|    %.6f                 |\n', rlt2,S(2));
str = fprintf('|                    |       %.6f    |
|    %.6f               |\n', Sum_rwi,Sum_rlwi);
fprintf('|-------------------------------------------------------------
------------------------|\n')

end

if Parameter==2
    rt1=input('1st retardation time: ');
    rw1=input('1st retardation weight: ');
    rt2=input('2nd retardation time: ');
    rw2=input('2nd retardation weight: ');
    a=[rt1;rw1;rt2;rw2;RVC;G1;n1];
    syms x
    f=(-x*x)*((a(1)*a(2))/(1+a(1)*x)+(a(3)*a(4))/(1+a(3)*x))*(a(5)-
1)+(x*a(5))+((a(6))/(a(7)));
    y=solve(f,x);
    solnvalue=double(y);
    rlt1=-1/(solnvalue(1));
    rlt2=-1/(solnvalue(2));
    rlt3=-1/(solnvalue(3));
    A=[(rlt1/(1-rlt1/rt1)) (rlt2/(1-rlt2/rt1)) (rlt3/(1-rlt3/rt1));
    (rlt1/(1-rlt1/rt2)) (rlt2/(1-rlt2/rt2)) (rlt3/(1-rlt3/rt2));
    rlt1 rlt2 rlt3];
    B=[0;0;n1/G1];
    S=inv(A)*B;
    Sum_rlwi=S(1)+S(2)+S(3);
    Sum_rwi=rw1+rw2;
    fprintf('|-------------------------------------------------------
----------------------------|\n')
fprintf('| Retardation time |Retardation weight|   Relaxation time   |
Relaxation weight     |\n');
str = fprintf('|        %.6f    |       %.6f      |    %.6f          |
%.6f                 |\n', rt1,rw1,rlt1,S(1));
str = fprintf('|        %.6f    |       %.6f      |    %.6f          |
%.6f                 |\n', rt2,rw2,rlt2,S(2));
str = fprintf('|                    |                  |     %.6f
|    %.6f                 |\n', rlt3,S(3));
str = fprintf('|                    |       %.6f    |
|    %.6f               |\n', Sum_rwi,Sum_rlwi);
fprintf('|-------------------------------------------------------------
------------------------|\n')

end

if Parameter==3
    rt1=input('1st retardation time: ');
    rw1=input('1st retardation weight: ');
    rt2=input('2nd retardation time: ');
    rw2=input('2nd retardation weight: ');
    rt3=input('3rd retardation time: ');
    rw3=input('3rd retardation weight: ');
    a=[rt1;rw1;rt2;rw2;rt3;rw3;RVC;G1;n1];
```

```
    syms x
    f=(-
x*x)*((a(1)*a(2))/(1+a(1)*x)+(a(3)*a(4))/(1+a(3)*x)+(a(5)*a(6))/(1+a(
5)*x))*(a(7)-1)+(x*a(7))+((a(8))/(a(9)));
    y=solve(f,x);
    solnvalue=double(y);
    rlt1=-1/(solnvalue(1));
    rlt2=-1/(solnvalue(2));
    rlt3=-1/(solnvalue(3));
    rlt4=-1/(solnvalue(4));
    A=[(rlt1/(1-rlt1/rt1)) (rlt2/(1-rlt2/rt1)) (rlt3/(1-rlt3/rt1))
(rlt4/(1-rlt4/rt1));
    (rlt1/(1-rlt1/rt2)) (rlt2/(1-rlt2/rt2)) (rlt3/(1-rlt3/rt2))
(rlt4/(1-rlt4/rt2));
    (rlt1/(1-rlt1/rt3)) (rlt2/(1-rlt2/rt3)) (rlt3/(1-rlt3/rt3))
(rlt4/(1-rlt4/rt3));
    rlt1 rlt2 rlt3 rlt4];
    B=[0;0;0;n1/G1];
    S=inv(A)*B;
    Sum_rlwi=S(1)+S(2)+S(3)+S(4);
    Sum_rwi=rw1+rw2+rw3;
    fprintf('|-----------------------------------------------------
----------------------------|\n')
fprintf('| Retardation time |Retardation weight|   Relaxation time  |
Relaxation weight     |\n');
str = fprintf('|       %.6f   |       %.6f     |   %.6f         |
%.6f                |\n', rt1,rw1,rlt1,S(1));
str = fprintf('|       %.6f   |       %.6f     |   %.6f         |
%.6f                |\n', rt2,rw2,rlt2,S(2));
str = fprintf('|       %.6f   |       %.6f     |   %.6f         |
%.6f                |\n', rt3,rw3,rlt3,S(3));
str = fprintf('|                    |                  |    %.6f
|   %.6f               |\n', rlt4,S(4));
str = fprintf('|                    |       %.6f   |
|   %.6f              |\n', Sum_rwi,Sum_rlwi);
fprintf('|-----------------------------------------------------------
-------------------------|\n')

end

if Parameter==4
    rt1=input('1st retardation time: ');
    rw1=input('1st retardation weight: ');
    rt2=input('2nd retardation time: ');
    rw2=input('2nd retardation weight: ');
    rt3=input('3rd retardation time: ');
    rw3=input('3rd retardation weight: ');
    rt4=input('4th retardation time: ');
    rw4=input('4th retardation weight: ');
    a=[rt1;rw1;rt2;rw2;rt3;rw3;rt4;rw4;RVC;G1;n1];
    syms x
    f=(-
x*x)*((a(1)*a(2))/(1+a(1)*x)+(a(3)*a(4))/(1+a(3)*x)+(a(5)*a(6))/(1+a(
5)*x)+(a(7)*a(8))/(1+a(7)*x))*(a(9)-1)+(x*a(9))+((a(10))/(a(11)));
    y=solve(f,x);
    solnvalue=double(y);
    rlt1=-1/(solnvalue(1));
    rlt2=-1/(solnvalue(2));
```

```
    rlt3=-1/(solnvalue(3));
    rlt4=-1/(solnvalue(4));
    rlt5=-1/(solnvalue(5));
    A=[(rlt1/(1-rlt1/rt1)) (rlt2/(1-rlt2/rt1)) (rlt3/(1-rlt3/rt1))
(rlt4/(1-rlt4/rt1)) (rlt5/(1-rlt5/rt1));
    (rlt1/(1-rlt1/rt2)) (rlt2/(1-rlt2/rt2)) (rlt3/(1-rlt3/rt2))
(rlt4/(1-rlt4/rt2)) (rlt5/(1-rlt5/rt2));
    (rlt1/(1-rlt1/rt3)) (rlt2/(1-rlt2/rt3)) (rlt3/(1-rlt3/rt3))
(rlt4/(1-rlt4/rt3)) (rlt5/(1-rlt5/rt3));
    (rlt1/(1-rlt1/rt4)) (rlt2/(1-rlt2/rt4)) (rlt3/(1-rlt3/rt4))
(rlt4/(1-rlt4/rt4)) (rlt5/(1-rlt5/rt4));
rlt1 rlt2 rlt3 rlt4 rlt5];
    B=[0;0;0;0;n1/G1];
    S=inv(A)*B;
    Sum_rlwi=S(1)+S(2)+S(3)+S(4)+S(5);
    Sum_rwi=rw1+rw2+rw3+rw4;
    fprintf('|-------------------------------------------------------
----------------------------|\n')
fprintf('| Retardation time |Retardation weight|   Relaxation time   |
Relaxation weight     |\n');
str = fprintf('|       %.6f   |       %.6f     |   %.6f         |
%.6f                |\n', rt1,rw1,rlt1,S(1));
str = fprintf('|       %.6f   |       %.6f     |   %.6f         |
%.6f                |\n', rt2,rw2,rlt2,S(2));
str = fprintf('|       %.6f   |       %.6f     |   %.6f         |
%.6f                |\n', rt3,rw3,rlt3,S(3));
str = fprintf('|       %.6f   |       %.6f     |   %.6f         |
%.6f                |\n', rt4,rw4,rlt4,S(4));
str = fprintf('|                  |                  |    %.6f
|   %.6f                |\n', rlt5,S(5));
str = fprintf('|                  |       %.6f   |
|   %.6f              |\n', Sum_rwi,Sum_rlwi);
fprintf('|-------------------------------------------------------
------------------------|\n')

end

if Parameter==5
    rt1=input('1st retardation time: ');
    rw1=input('1st retardation weight: ');
    rt2=input('2nd retardation time: ');
    rw2=input('2nd retardation weight: ');
    rt3=input('3rd retardation time: ');
    rw3=input('3rd retardation weight: ');
    rt4=input('4th retardation time: ');
    rw4=input('4th retardation weight: ');
    rt5=input('5th retardation time: ');
    rw5=input('5th retardation weight: ');
    a=[rt1;rw1;rt2;rw2;rt3;rw3;rt4;rw4;rt5;rw5;RVC;G1;n1];
    syms x
    f=(-
x*x)*((a(1)*a(2))/(1+a(1)*x)+(a(3)*a(4))/(1+a(3)*x)+(a(5)*a(6))/(1+a(
5)*x)+(a(7)*a(8))/(1+a(7)*x)+(a(9)*a(10))/(1+a(9)*x))*(a(11)-
1)+(x*a(11))+((a(12))/(a(13)));
    y=solve(f,x);
    solnvalue=double(y);
    rlt1=-1/(solnvalue(1));
    rlt2=-1/(solnvalue(2));
```

```
    rlt3=-1/(solnvalue(3));
    rlt4=-1/(solnvalue(4));
    rlt5=-1/(solnvalue(5));
    rlt6=-1/(solnvalue(6));
    A=[(rlt1/(1-rlt1/rt1)) (rlt2/(1-rlt2/rt1)) (rlt3/(1-rlt3/rt1))
(rlt4/(1-rlt4/rt1)) (rlt5/(1-rlt5/rt1)) (rlt6/(1-rlt6/rt1));
    (rlt1/(1-rlt1/rt2)) (rlt2/(1-rlt2/rt2)) (rlt3/(1-rlt3/rt2))
(rlt4/(1-rlt4/rt2)) (rlt5/(1-rlt5/rt2)) (rlt6/(1-rlt6/rt2));
    (rlt1/(1-rlt1/rt3)) (rlt2/(1-rlt2/rt3)) (rlt3/(1-rlt3/rt3))
(rlt4/(1-rlt4/rt3)) (rlt5/(1-rlt5/rt3)) (rlt6/(1-rlt6/rt3));
    (rlt1/(1-rlt1/rt4)) (rlt2/(1-rlt2/rt4)) (rlt3/(1-rlt3/rt4))
(rlt4/(1-rlt4/rt4)) (rlt5/(1-rlt5/rt4)) (rlt6/(1-rlt6/rt4));
(rlt1/(1-rlt1/rt5)) (rlt2/(1-rlt2/rt5)) (rlt3/(1-rlt3/rt5)) (rlt4/(1-
rlt4/rt5)) (rlt5/(1-rlt5/rt5)) (rlt6/(1-rlt6/rt5));
rlt1 rlt2 rlt3 rlt4 rlt5 rlt6];
    B=[0;0;0;0;0;n1/G1];
    S=inv(A)*B;
    Sum_rlwi=S(1)+S(2)+S(3)+S(4)+S(5)+S(6);
    Sum_rwi=rw1+rw2+rw3+rw4+rw5;
    fprintf('|-------------------------------------------------------
----------------------------|\n')
fprintf('| Retardation time |Retardation weight|   Relaxation time  |
Relaxation weight     |\n');
str = fprintf('|       %.6f   |       %.6f     |   %.6f         |
%.6f                |\n', rt1,rw1,rlt1,S(1));
str = fprintf('|       %.6f   |       %.6f     |   %.6f         |
%.6f                |\n', rt2,rw2,rlt2,S(2));
str = fprintf('|       %.6f   |       %.6f     |   %.6f         |
%.6f                |\n', rt3,rw3,rlt3,S(3));
str = fprintf('|       %.6f   |       %.6f     |   %.6f         |
%.6f                |\n', rt4,rw4,rlt4,S(4));
str = fprintf('|       %.6f   |       %.6f     |   %.6f         |
%.6f                |\n', rt5,rw5,rlt5,S(5));
str = fprintf('|                  |                  |    %.6f
|   %.6f               |\n', rlt6,S(6));
str = fprintf('|                  |       %.6f   |
|   %.6f             |\n', Sum_rwi,Sum_rlwi);
fprintf('|-------------------------------------------------------------
------------------------|\n')

end
```